Curcumin-loaded low-energy nanoemulsions as a prototype of multifunctional vehicles for different administration routes: physicochemical and *in vitro* peculiarities important for dermal application

Ines Nikolic, Dominique Jasmin Lunter, Danijela Randjelovic, Ana Zugic, Vanja Tadic, Bojan Markovic, Nebojsa Cekic, Lada Zivkovic, Dijana Topalovic, Biljana Spremo-Potparevic, Rolf Daniels, Snezana Savic

PII: S0378-5173(18)30648-3
DOI: https://doi.org/10.1016/j.ijpharm.2018.08.060
Reference: IJP 17746

To appear in: *International Journal of Pharmaceutics*

Received Date: 28 May 2018
Revised Date: 21 August 2018
Accepted Date: 31 August 2018

Please cite this article as: I. Nikolic, D. Jasmin Lunter, D. Randjelovic, A. Zugic, V. Tadic, B. Markovic, N. Cekic, L. Zivkovic, D. Topalovic, B. Spremo-Potparevic, R. Daniels, S. Savic, Curcumin-loaded low-energy nanoemulsions as a prototype of multifunctional vehicles for different administration routes: physicochemical and *in vitro* peculiarities important for dermal application, *International Journal of Pharmaceutics* (2018), doi: https://doi.org/10.1016/j.ijpharm.2018.08.060

Curcumin-loaded low-energy nanoemulsions as a prototype of multifunctional vehicles for different administration routes: physicochemical and *in vitro* peculiarities important for dermal application

Ines Nikolic[a], Dominique Jasmin Lunter[b], Danijela Randjelovic[c], Ana Zugic[d], Vanja Tadic[d], Bojan Markovic[e], Nebojsa Cekic[f], Lada Zivkovic[g], Dijana Topalovic[g], Biljana Spremo-Potparevic[g], Rolf Daniels[b], Snezana Savic[a*]

[a] Department of Pharmaceutical Technology and Cosmetology, Faculty of Pharmacy, University of Belgrade, 11221 Belgrade, Serbia

[b] Institut für Pharmazeutische Technologie, Eberhard-Karls Universität, D-72076 Tübingen, Germany

[c] Institute of Chemistry, Technology and Metallurgy, Department of Microelectronic Technologies, University of Belgrade, 11000 Belgrade, Serbia

[d] Institute for Medicinal Plant Research "Dr Josif Pančić", 11000 Belgrade, Serbia

[e] Department of Pharmaceutical Chemistry, Faculty of Pharmacy, University of Belgrade, 11221 Belgrade, Serbia

[f] Faculty of Technology, University of Niš, Leskovac 16000, Serbia

[g] Department of Biology and Human Genetics, Faculty of Pharmacy, University of Belgrade, 11221 Belgrade, Serbia

*Corresponding author: Dr Snežana Savić, Department of Pharmaceutical Technology and Cosmetology,
Faculty of Pharmacy, University of Belgrade, Vojvode Stepe 450, 11221 Belgrade, Serbia

Tel.: +381-11-3951366; Fax: +381-11-3972840

E-mail address: snexs@pharmacy.bg.ac.rs (S. Savić)

1. *Introduction*

In the past years an interest in the nanotechnology-based approach in designing carriers for drug molecules, cosmetic and food ingredients, has notably arisen (Vacchione et al, 2014; Klang and Valenta, 2011; Qian and McClements, 2011)). In the pharmaceutical field of application, general goal is to improve and strengthen prevention, diagnosis and treatment strategies of diseases, which could be accomplished by taking advantage of specific properties of the nanosized drug delivery systems (Klang and Valenta, 2011). Despite this fact, their market availability is still limited (Mu *et al*, 2018). In addition, intensive research in this field ought to be strongly supported by improved wide-spectrum methods of their characterization.

With the idea to provide appropriate level of active molecules at the application and/or action sites, a huge effort has been made to develop carriers with adequate characteristics. In this context, low-energy nanoemulsion may be prospective candidates. High solubilization capacity for hydrophobic actives, protection for unstable compounds, enhanced delivery and tissue penetrating properties, associated with good stability and relative easiness of preparation represent physicochemical and biological benefits of low-energy nanoemulsions, posting them among many other colloidal vehicles that have emerged (Đekić and Primorac, 2017; Uson *et al*, 2004). In general, nanoemulsions are defined as thermodynamically unstable mixtures of oil and water, with one of the liquids being dispersed in the other one, forming very small, submicron droplets, stabilized by a surfactant. They can be *water-in-oil* or *oil-in-water,* but the latter ones are more commonly used as drug carriers, aiming to encapsulate lipophilic drugs in aqueous environment (McClements, 2012). Existing methodologies for nanoemulsion preparation are divided into two essentially different approaches: high-energy and low-energy methods. On the one hand, high-energy production methods require special equipment and, consequently, they are

more expensive. Due to the high energy input, they can provide nanoemulsions with sufficiently small dispersed droplets and with very narrow size distribution using low surfactant concentrations (Vecchione,*et al*, 2016; Isailovic *et al*, 2017). On the other hand, low-energy ones rely on intrinsic properties of, primary, surface active ingredients to lower the interfacial tension and produce nanodroplets. Mild preparation conditions are favorable for encapsulation of fragile active molecules, and higher surfactant content compared to the high-energy nanoemulsions provides higher solubilization capacity for extremely hydrophobic actives. Even though they eventually follow identic mechanism, three possible low-energy methods for producing nanoemulsions are established: spontaneous emulsification, phase inversion temperature, and emulsion phase inversion (Komaiko and McClements, 2016; Anton and Vandamme, 2009). ~~The real advantage of the low-energy nanoemulsions lays in their suitability for encapsulating fragile molecules, coupled with moderate surfactant content compared to some similar carriers, often confused with – microemulsions (Anton et Vandamme, 2009). It is useful to underline that in spite of clear and defined differences, the misunderstanding of these emulsion systems with nanostructure could still be encountered.~~

Alongside (nano)technological development, an evident general interest in plant-based medicine and natural sources of medicinal compounds has been noted. In this view, curcumin represents a phytochemical compelling for therapeutic use due to its multifunctionality and pharmacological safeness. Curcumin and turmeric extract rich in this compound, derived from the rhizome of the *Curcuma spp*. (*Zingiberaceae*), have been the subject of many research papers discussing its antimicrobial, anti-inflammatory, antioxidant, cancer chemopreventive and, especially, potential chemotherapeutic properties, indicating its selective toxicity and safeness toward normal cells.

These findings rely on its extensive traditional use, afterwards supported by intensive research and clinical trials, which is well documented (Banejree *et al*, 2018; Seca and Pinto, 2018; Fotticchia *et al*, 2017; Vecchione et al, 2016; Gupta *et al*, 2013; Hatcher *et a*l, 2008; Sharma *et al*, 2005). However, this pleiotropic potential of curcumin encounters many difficulties: problematic solubility, physicochemical instability, rapid metabolism, and poor penetration and targeting efficacy, with low bioavailability as a consequence (Yallapu *et al*, 2015). This should be pointed out, as it makes curcumin extremely hard to work with, challenging researchers to develop formulations able to enhance biopharmaceutical performances of this molecule.

Therefore, in the scope of this work was development and investigation of nontoxic and multifunctional nanocarrier, with characteristics that are good enough to meet the expectations regarding drug loading capacity, effectiveness, stability, and technical requirements for their preparation, with a palette of possible application possibilities, representing a contemporary direction in the formulation approach. Considering low-energy nanoemulsion as prospective carriers, capable of attenuating obstacles imposed by curcumin, the present study aimed to investigate their formation via spontaneous emulsification method, using a combination of biocompatible surfactants as stabilizers. Having in mind some advantages provided by the skin as administration rout, coupled with increasing attention for nanocarriers intended for dermal drug delivery (Neubert, 2011), this was done with reference to potential topical application, but not exclusively limited to this way of administration. Dermal application of curcumin has become interesting because extensive evidences have been accumulated highlighting its beneficial activities in various skin-related disorders, such as photocarcinogenesis, photoaging, sunburns, diabetic wounds... Development of this kind of nanocarrier may represent a potential treatment modality for different skin disorders, improving the stability and effectiveness of this

molecule (Fotticchia *et al*, 2017; Yllapu *et al*, 2015; Kant *et al*, 2015; Kant *et al*, 2014).

As literature lacks the in-depth data on this topic (Singh *et al*, 2017; Komaiko and McClements, 2014), one goal was to contribute to better understanding these systems, providing a new knowledge on the generation of these multifunctional vehicles. This part may represent a special value of our work. For this purpose, a profound structural analysis was performed using sophisticated techniques and linking complementary pieces of information. To the best of our knowledge, these data have not been provided before in this form.

Furthermore, the other part of the study was devoted to selection of optimal low-energy nanoemulsion formulations as carriers for curcumin, compromising between the surfactant level and desired properties of the formulation. In this part, after the physicochemical properties and stability had been assessed, safety profile evaluation was carried out, as a proof of high biocompatibility of developed carriers. We would also like to stress the care for curcumin's stability evaluation, as it appears that it has been somehow neglected in the literature. Finally, the purpose of the last part was to analyze *in vitro* release kinetics of curcumin from selected vehicles, followed by efficacy assessment through *in vitro* antioxidant and antigentoxic potential tests. The latter one represents a contribution to biological evaluation of curcumin-loaded formulations. As oxidative stress is the key etiopathogenetic factor in development of various diseases, antioxidant, genoprotective as well as genoreparative activity of curcumin are important not only in prevention, but also in the treatment of skin disorders. This experimental section should serve to scratch deeper under the surface, paving a road for further work in determination of therapeutic implications of dermal application of curcumin.

2. *Materials and Methods*

2.1.Materials

Curcumin and Polysorbate 80 and were purchased from Sigma–Aldrich Co. (St. Louis, MO, USA), soybean lecithin (LE) was provided by Lipoid GmbH (Ludwigshafen, Germany), and medium chain triglycerides (MCT) were purchased from Fagron GmbH & KG (Barsbüttel, Germany). Ultrapure water (W) was obtained from the Gen Pure apparatus (TKA Wasseranfbereitungs system GmbH, Neiderelbert, Germany). All other used chemicals were of pharmaceutical or HPLC grade and used as received, without further purification.

2.2.Methods

2.2.1. Phase behavior investigation

Phase behavior of the system consisting of Polysorbate 80 as surfactant, soybean lecithin as cosurfactant, medium-chain triglycerides as the oil phase, and ultrapure water as the water phase was examined at room temperature, while surfactant to cosurfactant ratio was kept constant – 9:1, giving the final HLB of the surfactant-cosurfactant blend (SCoS) around 14. Lecithin was dissolved in the oil phase, and after the addition of Polysorbate 80, it was proceeded with mixing under magnetic stirrer for 30 minutes. Different *surfactant-to-oil ratios* (SORs) were prepared: 0.25, 0.5, 0.75, 1, 1.5, 2, 4, 9. In order to be more precise in determining SOR values adequate for low-energy nanoemulsion formation under these conditions, the systems with growing share of water (from 10 % to 90 % *w/w*) for each SORs were prepared by adding SOR mixtures to the calculated amount of water dropwise under the constant magnetic stirring at 1000 rpm

(spontaneous emulsification method). Every change that could be observed by naked eye was noted (e.g. gelling, transparency, turbidity…).

All mixtures were first inspected visually, and then additionally characterized after 24 hours. Low-energy nanoemulsions were identified as opalescent or turbid systems with average droplet size below 200 nm, exhibiting Newton flow.

2.2.2. Low-energy nanoemulsion preparation

Based on the phase behavior investigation, and with the view to compromise among desirable physicochemical properties, good safety profile and solubilization capacity for curcumin, mixture of oil and surfactants with selected SOR value was prepared, and nanoemulsions were formed via spontaneous emulsification method: oil and surfactant blend were being added dropwise to the calculated amount of water under constant magnetic stirring at 1000 rpm. After the whole amount of the blend had been used, systems were under constant stirring during 1-hour period. In case of drug-loaded formulations, curcumin was firstly dissolved in the mixture of the oil phase and surfactants, and then added to the water phase as previously described.

After preparation, each low-energy nanoemulsion was packed in crimped glass bottle and stored at 25 ˚C.

2.2.3. Droplet size and size distribution analysis.

For the purpose of droplet size analysis, photon correlation spectroscopy (PCS) was carried out by Zetasizer NanoZS90 (Malvern Instruments Ltd., Worcestershire, UK). This technique provides intensity weighted mean diameter (Z-average diameter, Z-ave) and PDI as a measure of the particle size distribution. Prior to measurements, all samples were diluted with ultrapure water (1:500, *v/v*) in order to obtain optimum scattering intensity. The measurements were

performed at 25 °C using He-Ne laser with wavelength of 633 nm, at a fixed scattering angle of 90°. All measurements were performed in triplicate.

To detect potential presence of small fraction of larger emulsion droplets, laser diffraction (LD) was performed as complementary method, using a Malvern Mastersizer 2000 (Malvern Instruments Ltd, Worcestershire, UK), which provided volume weighted diameters d (0.5), d (0.9) and D [4,3] as relevant sizing parameters.

2.2.4. Zeta potential analysis

Zeta potential (ZP), as a measure of droplet surface charge and one of the long-term stability indicators, was determined through measurements of electrophoretic mobility of nanoemulsion droplets, afterward converted to ZP using Zetasizer Nano ZS90 (Malvern Instruments Ltd., Worcestershire, UK), coupled with in-built software. The measurements were conducted immediately after the dilution of samples (1:500, *v/v*) with ultrapure water, at 25 °C. Constant conductivity was adjusted to 50 µS/cm using 0.9% (*w/v*) sodium chloride solution. All measurements were performed in triplicate.

2.2.5. Rheological properties characterization

To confirm the Newton flow of selected samples, their rheological properties were evaluated using DV-III ULTRA Programmable Rheometer, with *Rheocalc software* v.4.3 (Brookfield Engineering Laboratories, Middlesboro USA), at speed range 20-200 rpm, and temperature 20 ± 1°C.

2.2.6. Electrical conductivity

Given that electrical conductivity values can provide the preliminary insight to the internal

structure of the sample being analyzed and to detect the point where water is the outer phase, these measurements were performed with gradual addition of water to the selected blends of oil and surfactants, preceding more sophisticated methods that are also intended for this purpose. Measurements were performed using the Sensio + EC 71 conductivity meter (Hach Lange GmbH, Germany), immersing the electrode directly into the sample, in triplicates, at 25° C.

2.2.7. pH value measurements

Not only that formulation's pH value is to be analyzed in the context of application rout, it is important for maintenance of drug molecule stability and effectiveness, as well. This parameter was determined at 25 °C, in triplicates, using HI9321 pH meter (Hanna Instruments Inc, Ann Arbor, Michigan).

2.2.8. Differential scanning calorimetry

In order to check the physical state of curcumin in the formulations and to capture possible interactions among formulation components and active molecule, thermal analysis of curcumin, every used excipient separately, and developed placebo and drug-loaded formulations was conducted applying differential scanning calorimetry (DSC), by Mettler DSC 820 apparatus (Mettler Toledo GmbH Analytical, Giessen, Germany). About 10 mg of the samples were placed in standard aluminium pans, hermetically sealed and subjected to the heating program from 25 °C to 200 °C with the heating rate of 2K/min, under constant nitrogen flow. An empty aluminum pan served as a reference. Thermoanalytical parameters were calculated using the Mettler Toledo STARe software.

Even though the temperature range of water evaporation from these systems can clearly be separated from other thermal events, possible influence of water peak on accuracy of obtained

results was avoided by additional recording of DSC thermograms of the samples after air-drying during 24-hour period, under same thermal conditions.

Additionally, to confirm the results on matter arrangement – distribution of the oil and water phase, obtained after electrical conductivity measurements, thermal analysis of selected blend of water and surfactants with gradual addition of water was analyzed in cooling mode – from 25 °C to -50 °C, at cooling rate of 10K/min.

2.2.9. Atomic force microscopy

To get a direct access into the microstructure of optimal low-energy nanoemulsions – to determine its morphological properties and to confirm data obtained on mean droplet size, atomic force microscopy was carried out applying AutoProbe CP-Research SPM (TM Microscopes-Bruker). For more details, please consult the supplementary material section.

2.2.10.Determination of solubilization capacity of curcumin in the formulation

For the purpose of determination of the maximum solubilization capacity of developed formulation for curcumin, systems with several different concentrations were made. Curcumin was dissolved in the mixture of oil and surfactants, and then the procedure was the same as with the blank formulations. Testing concentrations ranged from 1 mg/mL to 5 mg/mL. Upon preparation, all nanoemulsions were packed in the crimped bottles and left for 24 h at room temperature, in order to see whether precipitation would happen. Systems that seemed homogenous when looked at by naked eye, additionally were checked by polarization microscope and DSC for any undissolved drug particles.

2.2.11.Polarization microscopy

Polarization microscopy with Carl Zeiss ApoTome Imager Z1 microscope (Zeiss, Göttingen,

Germany), integrated with the AxioCam ICc1 camera and Axio Vision 4.6 software was used to check if any anisotropy could be seen in the formulations. A drop of a sample was placed on the microscope glass slides, and magnifications 200X and 400X were captured with cross-polarizer in bright field using wavelength (λ) plate, to detect birefringence. This procedure was performed three times for each analyzed sample.

Additionally, this technique was applied to screen what happens when water and mixture of oil and surfactants are brought to tight contact, as during formulation preparing. A simulation of water/oil-surfactants contact surface was performed: a drop of the oil-surfactant mixture was placed on the microscope glass slides, and then, a drop of water was added. Interaction was captured in already mentioned conditions.

2.2.12.*St*ability study of selected curcumin-loaded and corresponding blank formulations

With a view to evaluating the stability of selected low-energy nanoemulsions, they were stored during 3 months at room temperature (25˚C), protected from light, and at predetermined time points following parameters were measured: mean droplet size, polydispersity index, pH, electrical conductivity, and curcumin content. Their physical appearance was observed as well.

2.2.13.*In vitro* release study

As developed formulations are intended for dermal application, to determine liberation kinetics of curcumin from these systems, *in vitro* release study was performed using vertical diffusion cells – Franz cells (n=6; Gauer Glas, D-Püttlingen, Germany). Having in mind low solubility and instability of curcumin, after detailed consideration and its stability evaluation in various potential acceptor phases, ethanol 50 % *v/v* was chosen as the one that could provide adequate solubilization and prevent degradation. Each cell receptor chamber was filled with ethanol 50 % *v/v* (chamber volume: 12 mL; effective diffusion area: 2.01 cm^2), preheated to 32 ˚C.

Polycarbonate membranes (Nuclepore™, Whatman, Maidstone, United Kingdom; pore dimeter: 0.1 µm). Release study was performed during 6 hours. LC-MS/MS technique was used for curcumin content determination in all samples. Aiming to find the model that best describes the drug liberation profile from investigated samples, cumulative amounts of curcumin per unit area were assessed through several kinetic models. For detailed description of the procedure, please consult the supplementary material section.

2.2.14.Determination of curcumin concentration

Accurate and precise determination of curcumin content in the formulations, as well as during drug release study, was performed by liquid chromatography coupled with mass spectrometry (LC-MS/MS) technique. For more detail on the method, please consult the supplementary material section.

2.2.15. Investigation of antioxidant activity

In order to evaluate antioxidant activity of curcumin from developed formulations, two assays were conducted: DPPH (2, 2-diphenyl-1- picrylhydrazyl assay, for free-radical scavenging activity) and FRAP (as ferric ion reducing antioxidant power).

2.2.15.1. DPPH assay

Firstly, in order to check the free-radical scavenging activity of curcumin, different concentrations of curcumin were prepared in methanol (0.25, 0.1875, 0.125, 0.0625, and 0.03125 mg/mL). DPPH radical was also dissolved in methanol (0.1 mM), and 3.6 mL of this solution was mixed with 400 µL of each curcumin methanolic solution, resulting in fin al concentrations: 0.025, 0.01875, 0.0125, 0.00625 and 0.003125 mg/mL, so that the absorbance values ranging from 0.1 to 0.9 were covered. After 30 minutes of incubation at room temperature, in dark, the

absorbance was recorded at 517 nm using Varian Cary-100 UV–VIS spectrophotometer (Varian BV, Middelburg, Netherlands). The blank sample was prepared with 400 µL of methanol instead of curcumin solution. The percentage of inhibition was calculated using the following equation: $I = [(Ac-As)/Ac] \times 100;$ where I stands for inhibition percentage, A_c for absorbance of a blank sample, and A_s for absorbance of the test sample. The inhibition percentage was plotted against concentration of the samples, and IC_{50} values, as the mean value of three measurements, was determined by linear regression analysis. In order to compare the antioxidant activity of curcumin with some commonly used antioxidant, the same experiment was performed with tocopherol, which is not only a potent antioxidant, but also possesses a structural similarity with curcumin.

2.2.15.2. FRAP assay

This test is very convenient for assessment of drug molecule antioxidative power from the hydrophilic formulation, as it is performed in aqueous environment, and it does not disturb the microstructure of the carrier. Briefly, a 100 µL of diluted nanoemulsion (in water) was mixed with 3 mL of freshly prepared FRAP reagent (25 mL of 300 mM acetate buffer (pH 3.6); 2.5 mL of 10 mM TPTZ (2,4,6-tripyridyl-*s*-triazine) solution in 40 mM HCl; 2.5 mL of 20 mM $FeCl_3$x6H2O solution in purified water), and then let to incubate for 30 minutes, at controlled temperature (37 ˚C). After this period, the absorbance was recorded at 593 nm, using Varian Cary-100 UV–VIS spectrophotometer (Varian BV, Middelburg, Netherlands). The blank was prepared and treated in the same manner, but it contained 100 µL of the same dilution of the placebo nanoemulsion (containing no curcumin). For comparison, this test was also performed with pure curcumin. As it is practically insoluble in water, the corresponding concentration of curcumin was prepared in methanol. So, the blank sample was also prepared by combining 100

μL of methanol with FRAP reagent. FRAP value was calculated based on the calibration curve of $FeSO_4x7H_2O$ standard solutions, covering the concentration range 25 μmol/L to 400 μmol/L, and expressed as mmol Fe^{2+}/g of dry matter. Concentration of $Fe_2SO_4x7H_2O$ was determined spectrophotometrically, so tested concentration of curcumin (0.1875 mg/mL) was selected based on absorbance intensity.

2.2.16.Genotoxicity potential evaluation – Comet assay

For safety profile assessment of selected formulations, their genotoxicity potential (ability to cause DNA damage) was evaluated through the Comet assay. Peripheral blood samples were collected in heparinized containers from 3 female volunteers (aged between 25 and 39 years, nonsmokers, they did not consume alcohol, receive any therapy, or take dietary supplements; samples from each subject were done in duplicate). Involvement of human volunteers was carried out in accordance with the Declaration of Helsinki. Each participant signed the informed consent for partaking in the experiment. Sample preparation, treatment and evaluation of the extent of DNA damage was conducted as in Zukovec Topalovic et *al*, 2015. For details on the experimental protocol, please consult the supplementary material section.

2.2.17.Antigenotoxic potential evaluation

Antigenotoxic activity, as a measure of curcumin's ability from developed formulations to protect DNA, or to repair it after induced damage, was evaluated through Comet assay as well, but in 2 different study designs: pretreatment and posttreatment protocol. The first one evaluates protective ability against oxidative induced DNA damage, whereas the latter one evaluates reparative features – ability to repair DNA after exposure to damaging agent. For details on the experimental protocol, please consult the supplementary material section.

2.2.18. Statistical analysis

Statistical analysis was conducted with the help of PASW Statistics software, version 18.0 (SPSS Inc., Chicago, USA). Whenever it was possible, results were presented as mean value of observed parameter ± SD. Statistical significances among multiple groups were evaluated though one-way ANOVA followed by Tukey's post hoc test. Assessment of statistical significance in the values of physicochemical parameters of low-energy nanoemulsions in stability study was performed through Student's t-test. The level of statistical significance was set at $p<0.05$.

3. Results and discussion

3.1. Phase behavior investigation

Phase behavior investigation was conducted in order to reach and determine the region of optimal surfactant-to-oil ratio for low-energy nanoemulsion formation for selected excipients (Polysorbate 80, soybean lecithin, medium-chain triglycerides). The idea was also to get an insight into the occurrence at the contact border of water and oil-surfactant mixture during spontaneous emulsification, lightening some fundamental aspects of low-energy nanoemulsions formation in this concrete case. This experimental part should provide exact information on inner phase origination through the process of spontaneous emulsification

During the investigation of the phase behavior it was observed that in cases with lower water content gelling was very pronounced phenomenon, implying that some anisotropic structures were formed, such as liquid crystals. Eventually, when samples contained more than 50 % *w/w* of water, they became easily flowable and liquid. The lowest SOR value that was able to give the low-energy nanoemulsion was around 0.75 for this system. Below this value only coarse emulsions appeared, milky white mixtures, with visible lagging on the glass, prone to the fast phase separation. By contrary, systems with SOR values 0.75 or higher were easily flowable,

without lagging, giving the impression of a smooth movement, with typical bluish reflection when inspected towards light. As it could be expected, the transparency grew along with the surfactant content (Figure 1)~~. (SOR value). Microemulsions, as isotropic and completely transparent systems, were formed only in the cases when surfactant reached the highest level - for SOR 9~~. In the case of the SOR (9:1), the surfactant concentration was high enough to form an oil-in-water microemulsion, isotropic and completely transparent system. It should be noted that even here semisolid liquid crystalline phase was formed during the contact of SOR mixture with water, but after the mixing procedure, the final formulation was completely transparent.

Literature suggests that, during spontaneous emulsification process, at the border of organic and water phase, a bicontinuous microemulsion is formed or, alternatively, liquid crystalline structures, but this has been poorly defined. Due to the stirring process, the breakup of these boundary formations is facilitated, and small droplets are formed (Komaiko and McClements, 2014; Komaiko and McClements 2016). Before going further, it is important to get a clearer image of what happens when surfactant-oil mixture and water are brought together. With this view, the simulation of their contact was performed and inspected. When a drop of surfactant and oil mixture is placed on ~~one~~ a microscope slide, and a drop of water next to it, after a few moments they get into a close contact, and at the boundary a turbidity is formed, implying that emulsification occurs. Spontaneous emulsification is a process that occurs without external energy, with the help of surface active components or cosolvents, when two immiscible liquids are brought in contact - without stirring, the blend becomes turbid. In general, the kinetics of this process is accelerated by a slight energy input (e.g. stirring), even though it is called spontaneous emulsification or even more loosely term is used – self-emulsification. But, it is worth noting that mechanisms that may be involved in this phenomenon are still, at some points, a matter of

discussion and not fully understood, in spite of the fact that this process was observed long time ago. Several mechanisms have been proposed so far (Lopes-Montilla *et al*, 2002):

1. interfacial turbulence,
2. negative interfacial tension,
3. diffusion and stranding.

The first two mechanisms involve the mechanical instability of the interface, whereas in the case of diffusion and stranding emulsification has a chemical origin, and it can happen even for quite high interfacial tensions. It usually happens in the systems where a component soluble in both phases is present, such as a cosolvent. This may be the case in our system, as Polysorbate 80 was used, a hydrophilic surfactant which can easily be mixed with oil. ~~Also,~~ In our emulsion preparation protocol, it is added in the oil phase and during the preparation, this amphiphilic component diffuses from the oil to the water phase, carrying with itself some small portions of oil. At the vicinity of interface, a three-component system (oil-surfactants-water) is formed, amphiphilic component diffuses further into the water phase, and as soon as water becomes supersaturated in oil, these small oil portions eventually become "stranded" in tiny droplets (Lopes-Montilla 2002, Saberi *et al*, 2013). Actually, this diffusion of a hydrophilic surfactant from the oil to the water phase represents the fundamental principle of the low-energy nanoemulsification process regardless the method (Antone and Vadame,2009).

~~In addition, it should be emphasized that, in case of this system, at the contact points of organic phase and water, a highly viscous phase is formed~~. In addition, it should be emphasized that at the contact points of organic phase (mixture of Polysorbate 80, soybean lecithin and medium-chain triglycerides) and water a highly viscous phase is formed. When observed under polarized

light, anisotropic structures could easily be seen (Figure 2a), suggesting that liquid crystalline phase is present here. This intermediate phase spreads rapidly, and eventually disintegrates. To throw more light to this phenomenon, surfactant-oil-water contact was observed under AFM. It is obvious that, when this viscous system is analyzed, "tubes and streams" are present (Figure 2b), probably due to the infiltration of one phase into the other and formation of liquid crystalline transition phase.

This is in line with some recently proposed mechanisms explaining the origin of spontaneous emulsification process by transitory formation of myelinic structures at the oil-water interface. These myelinic structures are in fact long tubes of highly viscous lamellar liquid crystalline phase, which finally "explodes" into small droplets after swelling in water (Lopes-Montilla 2002; Buchannan *et al*, 2000). Such an anisotropy was not detected in the samples of prepared low-energy nanoemulsions which were analyzed under polarized light, confirming that liquid crystalline phase truly is the transitory phase that appears at the contact surface of organic and water phase during spontaneous emulsification.

By all means, the process of spontaneous emulsification is more complex than it seems, governed by different mechanisms which are related to the system composition, physicochemical properties of the components and emulsification protocol (Keuneth *et al*, 1972; Lopes-Montilla *et al*, 2002).

3.2. Nanoemulsion selection and detailed physicochemical characterization

In order to find the most suitable ratio of nanoemulsion components for the prospective carrier, more detailed characterization was performed, coupling the formulation's properties with the needs of the model drug, having in mind the stability and safety issues in parallel.

~~In low-energy nanoemulsions, along with process parameters, composition plays a decisive role in formation and stability, especially regarding viscosity of the oil phase and its solubility in the water phase (Komaiko and McClements, 2016; Wooster *et al*, 2008).~~ In order to obtain a stable nanoemulsion, appropriate surfactant type and its concentration should be combined with adequate oil properties (low viscosity and aqueous insolubility) (Komaiko and McClements, 2016; Wooster *et al*, 2008). It should also be noted that spontaneous emulsification process applies to the systems with moderate dispersion phase volume - about 10 % (Lopes-Montilla, 2002).

Some comparative properties of selected nanoemulsions with different SOR values are summarized in Table 1.

It could easily be noted that there is a strong dependence of the mean droplet size on the surfactant concentration - the higher surfactant concentration, the lower droplet size. This is expected as surfactant is directly responsible for lowering the interfacial tension, and when it is present in much higher portion than the oil, it gives rise to smaller oil droplet formation (Tadors *et al*, 2004). ~~Also, if the SOR is higher, then there is a greater probability that the interface is saturated, and SOR value is closely related to the triggering process of spontaneous emulsification (Antone and Vandame, 2009).~~ In addition, if SOR value is high enough (close to 1 or higher), then there is a greater probability that the interface is saturated with stabilizer's molecules. Not only that this is important in the context of stability, but it is also closely related to the triggering process of spontaneous emulsification. As in low-energy methods no high energy input is provided, the only driving force for emulsification is surfactant's ability to lower the oil-water interfacial tension and enable their mixing (Antone and Vandame, 2009).

When PDI is analyzed, at the beginning, PDI decreases with increase in SOR value. But, after

SOR 1, there is a visible and well-established trend – PDI values are higher in the formulations with higher surfactant concentration, underlying wider droplet size distribution in these cases. Presumably, when more surfactant is available, then a few populations of smaller droplets may form, resulting in inhomogeneous size distribution. ~~There is a general hypothesis that this is unfavorable regarding long-term stability of (low-energy) nanoemulsions because systems with wider droplet size distribution are more susceptible to the Ostwald ripening destabilization process. Moreover, the possibility of micelle formation in the situations when surfactant is present in much larger portion than the oil cannot be neglected. The population of micelles may not only contribute to the PDI increase, but also accelerates the Ostwald ripening (Tadros *et al*, 2004).~~ On the one hand, there is a general hypothesis that this is unfavorable regarding long-term stability of (low-energy) nanoemulsions because systems with wider droplet size distribution are more susceptible to the Ostwald ripening destabilization process (Tadros *et al*, 2004; Taylor, 1998; Kablanov and Shchukin, 1992). But on the other hand, emulsions with very low droplet size, efficiently stabilized by a surfactant layer, with low oil-water interfacial tension and composed of oils that are inherently insoluble in the aqueous phase, are more resistant against this destabilization process (Helgeson, 2016; Taylor, 1998). However, the possibility of micelle formation in surfactant's surplus cannot be neglected. The micelle population may increase the PDI as well and influence Ostwald ripening (Tadros *et al*, 2004).

As these nanoemulsions were formulated with the idea to be prospective carriers for curcumin, the pH value was the parameter of high importance, closely related to the stability of this molecule, given that it is well known that curcumin exhibits rapid oxidative degradation in the alkaline conditions (Sharma *et al*, 2005; Wang *et al*, 1997). Basically, only formulations with pH below 7 were taken into consideration as prospective curcumin carriers.

Having in mind that the idea was to reach the compromise regarding the formulations' stability, their properties and solubilization capacity for curcumin on the one hand, and safety profile on the other hand, priority was given to the ones that have surfactant concentration as low as possible, but high enough to provide desirable characteristics. So, based on overall satisfying properties in terms of pH value, droplet size and size distribution, and acceptable surfactant concentration, formulation with SOR 1 and with 10% of the oil phase (F1, Table 2) was chosen for further estimation and curcumin incorporation.

Even though water is present in much higher portion than the oil and surfactant, in order to have a definite confirmation about the matter arrangement and internal structure, electrical conductivity and DSC measurements of SOR 1 mixture with gradual addition of water were performed, coupled with the AFM experiments.

Samples with low water content exhibited negligible electrical conductivity (Figure 3a), which is related to the formation of viscous liquid crystalline structures. In this area water droplets are most likely dispersed in this semisolid medium, with a merely slight interaction among them. Samples with higher water portion were followed by an intense increase in values of electrical conductivity due to the formation of water channels. A sharp change in the conductivity graph suggests that the system transits through a structural change. More precisely, the maximum electrical conductivity value was achieved at 60 % (*w/w*) of water, which refers to the fact that here water shifted towards the outer phase (Isailovic *et al*, 2017). This may imply that here ~~a formation a~~ water-continuous low-energy nanoemulsion formation took place. Starting from this point (60 % w/w of water, and more), sample apparently started to behave as an easily flowable liquid. A significant decrease in electrical conductivity after 80 % (*w/w*) of water content can be explained with the dilution of the system - being dominant component in terms of quantity, water

decreased the concentration of the dispersed phase, resulting in lower electrical conductivity values (Santana *et al*, 2012).

Furthermore, rheological properties of the samples with 60 %, 70 % and 80 % *w/w* water indicated that all of them belong to the Newton liquids – shear stress showed linear dependence on shear rate (Figure 3b) and, as expected, viscosity decreased along with increase of water fraction.

DSC measurements in cooling mode (Figure 4a) strongly supported findings based on electrical conductivity. Ultra-purified water (used in our experiments) showed an exothermic peak at -15 ˚C. Evidently, interactions of water with hydrophilic parts of the surfactant layer modified its thermodynamic behavior. In the samples with low water content, water is tied, resulting in the shift of the freezing point of water towards lower temperatures (Todosijevic *et al*, 2014). ~~In first samples, when water is present less than 30%, the water peak was even not detected.~~ The water peak was even not detected in the samples with less than 30% *w/w* of water. Apparently, with increase in water content, the peak was getting more and more pronounced, moving towards higher temperatures. Finally, in case of 80 % of water, the peak was large and sharp, corresponding, probably, to the "bulk" water. ~~At this point water is present in higher portion, giving the peak almost identic as the one for pure water. So, this leads us to conclusion that in the F1 formulation water is the outer phase.~~ At this point water is present in higher portion, giving the peak almost identic as the one for pure water, implying that in the F1 formulation water is the outer phase

In addition to this, to take a direct look at the inner microstructure of the F1 formulation, AFM images were captured (Figure 5). Irregular spherical droplets could be observed, with dimensions corresponding to those obtained with DLS measurements and laser diffraction. AFM confirmed

the morphology of dispersed phase which had previously been supposed, proving that small oil droplets are really generated as the inner phase during spontaneous emulsification. Interestingly, some fractions with smaller dimensions could also be noticed. It seems logic that they belong to the surfactant aggregates that were formed simultaneously with the dispersed and stabilized oil droplets (Anton and Vandame, 2009). Nevertheless, this should be confirmed with other experimental techniques.

3.3.Determination of solubilization capacity for curcumin in the formulation and characterization of curcumin-loaded low-energy nanoemulsions

Given that there is no established therapeutic concentration of curcumin for topical application, the goal was to evaluate the maximum solubilization capacity of the chosen formulation for curcumin. For this purpose, apart from blank (F1) low-energy nanoemulsion, several formulations with different curcumin content were prepared – formulations with 1 mg/mL, 2 mg/mL, 3 mg/mL, 4mg/mL and 5 mg/mL. Having incorporated curcumin in the low-energy nanoemulsions in various concentrations, they were let to equilibrate for 24 hours, and then visually inspected. Easily visible curcumin precipitation occurred in the formulations with 4mg/mL and 5 mg/mL (Figure 6). The first three formulations, when looked at bare eye, seemed homogenous. In order to confirm this and to define surely the physical state of the drug in the formulation, DSC thermograms of pure curcumin and curcumin-loaded formulation with 1 mg/mL, 2mg/mL and 3mg/mL of curcumin (named F1_CU_1, F1_CU_2 and F1_CU_3, respectively; Table 2) were analyzed. On the one hand, as it can be seen in the Figure 4b, curcumin gives rise to a sharp peak corresponding to its melting point, which demonstrates its crystalline structure. On the other hand, this peak was absent in the DSC thermograms of curcumin-loaded low-energy nanoemulsions (Figure 4b). DSC thermograms of both blank and

curcumin-loaded formulations revealed only an intense endothermic peak corresponding to the water evaporation (Figures 4b and 4c). These experiments did not discover any undissolved drug crystals in the analyzed material, implying that it is completely solubilized and molecularly dispersed in the carrier. The finding was confirmed by DSC curves of air-dried samples and supported by polarization microscopy of drug-loaded formulations – no curcumin crystals were detected. Interestingly, the shift of the water peak towards lower temperatures with increase of curcumin content in the formulations could be observed, which might be related to the interactions of curcumin's hydroxyl groups with the hydrophilic part of the interface, causing some rearrangements in this region. Similar findings were discussed elsewhere (Sreekanth and Bajaj, 2013; Chen *et al*, 2012; Li *et al*, 2017).

Comparative physicochemical properties of the blank formulation and drug-loaded ones are presented in the Table 3. Curcumin presence in the formulation induced significant Z-ave augmentation compared to the blank formulation, and this augmentation was proportionate to its concentration - the formulation with the highest curcumin concentration (F1_CU_3) exhibited the greatest Z-ave augmentation. ~~Sizing experiments with laser diffraction did not detect any droplet bigger that 200 nm.~~ Sizing experiments with laser diffraction did not detect any droplet diameter crossing 200 nm. For more details, please consult the supplementary material section. pH increased, but it remained in acidic range, which should maintain curcumin's stability in the formulation. On the contrary, ZP reduced significantly, as well as electrical conductivity. Such findings may be connected to the fact that at pH 3-7 curcumin acts as an extremely potent H-atom donor (Sharma *et al*, 2005), thus keeping phospholipids (lecithin) from ionization. Even though electrostatic repulsion is not the main stabilization mechanism in this case, ZP values were measured in order to have a clue about the surface charge properties as an indication of

long-term stability of these formulations. In general, when talking about electrostatic stabilization, absolute ZP values above 30 mV suggest good kinetic stability (Müller *et al*, 2012). However, this should not be taken strictly, because here electrostatic stabilization that originates from the lecithin molecules at the interface only partially contributes to the nanoemulsion stabilization, because steric stabilizer (Polysorbate 80) is present in much higher portion. Owing to its adsorption, during ZP measurements, the diffuse layer is protected from removal while the sample moves in the electrical field. As a result, the shear plane is shifted further away from the droplet surface, so ZP is then measured farther from the Stern layer. Due to the exponential decay of the potential in the diffuse layer, the measured ZP is lower than in dispersions without steric stabilizers (Pardeike and Müller, 1996). It has been reported that in a combined electrostatic and steric stabilization ZP values of about |−20 mV| should be sufficient for physical stability (Jacobs and Müller, 2002). So, slightly lower absolute ZP values than 30 mV should not be worrying. Moreover, curcumin did not alter rheological properties of the formulation – they preserved Newton flow.

3.4. Release kinetics study of curcumin from developed formulations

As our formulations are intended for topical application, *in vitro* release study of curcumin from the F1_CU1, F1_CU2 and F1_CU3 low-energy nanoemulsions was performed in vertical diffusion cells (Franz cells). Although physicochemical characterization can be profound and provide useful information on the structure of a vehicle, drug-vehicle interactions, or even localization of its components, it cannot predict drug molecule release kinetics. Having in mind that release is a *condition sine qua non* for absorption by the skin and any expected effect, analysis of the kinetics of this process should be an important part of the system evaluation. ~~But~~ Nvertheless, it should be kept in mind that this study can be taken only as an indication and a

tool to detect the influence of various formulation aspects on drug release from the formulation, and not as a direct proof of (bio)availability (Shah *et al*, 2015; Isailovic *et al*, 2017).

Being aware of curcumin's chemical instability, it was quite a demanding task to adjust the testing protocol to this molecule. Even though it is well known that curcumin is prone to rapid oxidative degradation under pH above 7, in majority research paper this information is neglected and release studies were performed with PBS 7.4, which is absolutely inadequate choice in this case. In our study, release kinetics was estimated in ethanol-water mixture (50 % v/v of ethanol in purified water), as it appeared to be the most suitable, not only in terms of curcumin's stability, but also regarding satisfying solubilization capacity. For details on the stability evaluation of curcumin in several receiver media, please consult the supplementary material section.

As shown in the Figure 7, all investigated formulations exhibited a linear relationship between the cumulative amount of released curcumin per area unit and a square root of time, meaning that Higuchi diffusion model is the one that describes best the release kinetics of curcumin from these formulations. Not surprisingly, the highest released amount after 6 hours (at the end of the experiment) was obtained for the F1_CU_3, which was followed by F1_CU_2 and then F1_CU_1. Moreover, in all three cases about 10 % of the curcumin was released compared to the total curcumin content in the sample, suggesting that this molecule is highly immobilized in the inner phase, which prolongs its diffusion. When these results are being interpreted with regard to curcumin's extremely poor water solubility, they may also indicate that curcumin has difficulties to pass through the hydrophilic surrounding, which could be the limiting factor for its availability at the application site.

However, as stated earlier, this *in vitro* test is not able either to reflect the complexity of

interactions that take place at the application site or to predict the extent of penetration/permeation through the skin. Thus, additional experimental work should be performed using skin models in order to obtain information on curcumin's availability upon dermal application from these formulations.

3.5. Stability study of the blank and curcumin-loaded low-energy nanoemulsions

In order to estimate the physicochemical stability of prepared curcumin-loaded low-energy nanoemulsions and corresponding blank formulation, short term preliminary stability study during 3 months at room temperature was carried out. Parameters that were monitored are Z-ave, PDI, ZP, pH and EC, as well as visual appearance, and results are collectively shown in the Table 4. Furthermore, as the most valuable information, special attention was paid to curcumin content determination during this follow-up period.

After 3 months storage, all formulations were highly fluid with no visible signs of any physical instability – they looked as if they were just prepared. Absence of curcumin crystals was confirmed through polarization microscopy.

The mean droplet size of both placebo and curcumin-loaded low-energy nanoemulsions did not change appreciably. As PDI remained in desirable values – lower than 0.2, it suggested no droplet coalescence within this time.

It is known that lower pH levels of the systems can decrease lecithin ionization, and, as a consequence, lower absolute ZP values can be observed, leading to attenuation of electrostatic repulsion among droplets (Isailovic *et al*, 2016). Decrease in absolute ZP values was found only in the F1 formulation, probably due to the lower pH compared to those with curcumin. Nevertheless, this change was not significant.

Furthermore, neither electrical conductivity, nor pH changed in an unexpected manner. Even though electrical conductivity of the F1 decreased significantly, this should not be taken as an instability indication (Isailovic *et al*, 2016)

As curcumin is very prone to oxidative degradation, important finding was that it remained stable in the formulation during this follow-up period, which was one of the key challenges (Figure 8). It should be emphasized that many oxidation reactions occur at the vicinity of the interface of emulsion droplets (McClements and Decker 2000). In general, there has been a limited interest in the ability of emulsifiers to protect the bioactive compound encapsulated in the formulations, they have been selected usually based on their ability to enhance the physical stability of emulsions (Pan *et al*, 2013). ~~But,~~ Among many possibilities to enhance oxidative stability of the encapsulated unstable molecules, it is believed that, at higher surfactant concentrations, packing of the surfactant molecules at the oil-water interface is tighter, providing an efficient physical barrier to oxidative species. Alternatively, there are findings that support the opinion that excess of surfactant forms micelles in the aqueous phase which are able to encapsulate prooxidative species (McClements and Decker, 2000). Additionally, lecithin's potential to block permeation of peroxyl radicals across the interface of oil-in-water emulsion and to decrease the rate of oxidation of bioactive encapsulates has been proven (Pan *et al*, 2013). Presumably, these effects could not be neglected, along with appropriate pH environment that also hindered curcumin's degradation.

To sum up, both blank and curcumin-loaded low-energy nanoemulsions have not shown any proof of physical or chemical instability within 3 months storage at room temperature, indicating promising results in the future.

3.6. Evaluation of biologic activity of curcumin from developed formulations

Curcumin is well known for its chemopreventive properties, indicating the strong bond between the tumor biology and this natural compound with pleiotropic effects (Yallapu *et al* 2012). It can potentially prevent cancer development with no observed toxicity (Aggrawal *et al*, 2007), which sometimes seems too good to be true. Accordingly, our study was designed to offer an evidence line and demonstrate some aspects of prospective efficacy of curcumin from developed low-energy nanoemulsions. As it has been proved, there is a strong link between oxidative stress and cancer (Valko *et al*, 2006), so antioxidative activity of curcumin and drug-loaded formulations was determined, in line with antigenotoxic estimation.

3.6.1. Antioxidant activity

For the purpose of evaluation curcumin's efficacy as an antioxidant, two tests were performed (DPPH and FRAP), differing in the fundamental principal of antioxidant protection. On the one hand, DPPH assay is based on neutralization of DPPH free radical by hydrogen-donating antioxidant, followed by formation of DPPH-H in the reaction, which fades out the purple color of DPPH solution. The discoloration degree correlates to the antioxidant potential of the tested compound (Blois M, 1958). On the other hand, chemical basis of FRAP test is different – it relays on the capacity of the tested molecule to reduce the oxidative species through the electron transfer, which is, as in previous case, also followed by the change of the color (Benzie and Strain, 2009). In these experiments tocopherol was used as a standard, as it has similar chemical structure as curcumin and proven antioxidant activity.

In our DPPH experiment, curcumin showed IC_{50} value of 0.1187 mg/mL, whereas for tocopherol the value of 0.1097 mg/mL was recorded. No doubt, this result pointed out high antioxidative activity of curcumin. It is in accordance with the fact that keto form of curcumin acts as an

extremely potent hydrogen donor (Sharma *et al*, 2005), which is the prerequisite for this reaction. It was found that keto-enol-enolate equilibrium of the heptadienon structure, with highly activated carbon atom, is responsible for curcumin's antioxidant activity (Jovanovic *et al*, 1999). Dependence of DPPH absorbance on curcumin and tocopherol concentrations, as well as antioxidant activity of these molecules in different concentrations obtained in our experiment are shown in the Figures 9a and 9b. DPPH absorbance decay can be observed, and when calculated as percentage of antioxidant activity, linear relationship between curcumin concentration and antioxidant activity was obtained.

~~DPPH assay, as a variety of antioxidant evaluation tests, has a protocol that considers using organic solvents. Due to their ability to dissolve lipids and surfactants, this test is not suitable for evaluation of the antioxidant effects of the whole formulation, where the tested molecule is entrapped. It is evident that during the experiment, after the contact of the formulation and the DPPH solution in the organic solvent, carrier's structure is broken. Consequently, the determined effect comes from the released antioxidant molecule, and not from the formulation.~~ Standard antioxidant tests, such as DPPH, are usually performed in the environment which is unfriendly to the lipid-based formulations. Organic solvents, used in the protocol of these tests (e. g. ethanol, methanol), have the ability to dissolve lipids and surfactants. During the experiment, after the contact of the formulation and the DPPH solution in the organic solvent, carrier's structure becomes broken. Consequently, the determined effect comes from the released antioxidant molecule, and not from the formulation. So, it cannot be claimed that the antioxidant activity would be the same for the formulation. Though, this test could serve as an indication of the antioxidant's stability in the formulation. When the same DPPH experiment was performed with the low-energy nanoemulsions with curcumin (with fresh ones and with the ones stored at room

temperature during 3 months), similar results were obtained as when free molecule was tested, suggesting that antioxidant activity of curcumin was not altered when incorporated in the formulation, during the preparation steps or storage, and that it was stable in the formulation. Details are shown in the supplementary material section.

FRAP assay results are presented in the Figure 10c. As it can be seen, curcumin has higher FRAP value than tocopherol (1.19±0.02 mmol Fe^{2+}/g vs. 0.93±0.06 mmol Fe^{2+}/g). This electron-transfer antioxidant mechanism is related to the phenolic properties of the curcumin molecule, as it was also shown previously with other polyphenolic compounds (Zugic *et al*, 2015; Jovanovic *et al*, 1999).

Furthermore, FRAP test is suitable for assessment of antioxidant properties of developed curcumin-loaded formulations, as it is conducted in aqueous environment, without organic solvents, thus not disturbing their microstructure. Presumably, the effectiveness of a molecule with antioxidant activity can be different when applied within a formulation compared to a free form (e. g. as a solution). In addition, in order to have adequate comparison of FRAP values of free curcumin and curcumin-loaded low-energy nanoemulsions, formulations had to be diluted in water to obtain the same concentration. As it had to be in the range of concentrations for the calibration curve for $FeSO_4x7H_2O$, the chosen concentration in our case was 0.1875 mg/mL In our experimental setting, there was no observed significant difference between tested formulations and free curcumin (Figure 9c) - their FRAP values were comparable to the free curcumin in the same concentration, even though it was logic to expect lower/slower activity of the molecule that is entrapped in the formulation. ~~This may be explained by the fact that, as bibliography suggests, curcumin has moderate electron donating ability, and coupled with extremely low solubility in water (which is the preferable environment for this process), the~~

~~significance of electron-transfer aspect of antioxidant activity may be diminished (Jovanovic *et al*, 1999).~~ That is probably the reason why some pronounced difference was not noticed. Activity estimation and comparison should additionally be observed in long-term study, leaving a possibility to capture potentially improved/prolonged efficacy of curcumin from the formulation, which could be linked with the release kinetics of curcumin from the nanocarrier.

Blank formulation did not exhibit any detectable antioxidant activity.

Obtained results lead us to conclusion that curcumin is extremely potent and highly active antioxidant agent, expressing efficacy in low concentrations and able to stop oxidative species in two different mechanisms. Its activity was not altered when incorporated in the low-energy nanoemulsion. Despite strong entrapment within the formulation, it exhibited respectful activity. This is in line with the finding that, in terms of H-atom transfer reactions, curcumin appears to be better and much faster antioxidant even than some well-known H-atom donors, like thiols (Jovanovic *et al*, 1999).

3.6.2. Genotoxicity evaluation

In order to assess the safety profile of developed formulations, the Comet assay was performed on the whole blood treated cells. Based on our experimental results, the blank formulation did not cause significant DNA damage, compared to PBS as negative control. Moreover, curcumin-loaded formulations in all tested concentrations (1, 2 and 3 mg/mL) proved to be safe and nongenotoxic. They did induce slight increase in the number of cells with DNA damage compared to the blank formulation (Figure 10a), but it was close to control. Curcumin concentration in the tested range did not affect the level of the induction of DNA damage. Despite the fact that some studies showed that curcumin acts both as antioxidant and pro-oxidant agent toward red blood cells (Banerjee *et al*, 2008), and exerts genotoxic properties at higher

concentrations to human lymphocytes in *in vitro* models (Sebastia *et al*, 2012), which may be related to its effectiveness in proposed indications, no significant genotoxicity was noticed towards treated human whole blood cells in our study. As researchers suggest strong activity and interference of curcumin in many signaling pathways responsible for carcinogenesis (Villegas *et al*, 2008; Thangapazham *et al*, 2006), as well as genotoxic and cytotoxic effect of curcumin towards various types of cancer cells (Kumar *et al*, 2016; Yallapu *et al*, 2013), it is of high importance to evaluate this ability of curcumin not only solely, but also in combination with other chemicals, including chemotherapy drugs used in cancer treatment (Mendonca *et al*, 2009).

3.6.3. Antigenotoxic activity assessment

After biocompatibility of developed formulations had been proven, and in addition to powerful antioxidant performances that had been confirmed, antigenotoxic properties of curcumin-loaded formulations were assessed also through Comet assay, but now applying two different protocols (pretreatment and posttreatment) with a view to lightening some aspects of curcumin's mechanism of action.

Obtained results proved strong ability of developed formulations not only to protect DNA from oxidative damage, but also to repair already damaged cells (Figures 10a and 10b). Genoprotective property is certainly closely related to the antioxidant potential of curcumin and direct scavenging of peroxy-radicals. What is even more impressing, reparative capability towards treated cells seems intense suggesting that overall effect was not only due to direct chemical neutralization of free radicals, but also here the uptake of the molecule by the cells might have played a role (Banjeree *et al*, 2008). This could have been followed by the stimulation of antioxidant and reparative enzymes and maintenance of their activity during oxidative stress, as similar findings were reported for some other polyphenolic plant extracts

(Ghanema *et al*, 2012). In addition to this, an evidence of this concept is the fact that curcumin's ability to increase the intracellular concentration of reduced form of glutathione and regulation of gene expression and synthesis of different proteins involved in cellular response to environmental stress has been discussed and proved (Sharma *et al*, 2005).

Interestingly, even the blank formulation showed efficacy in attenuation of oxidative DNA damage, which can be connected with the findings that lecithin shows antioxidant activity (Pan *et al*, 2013), enabling antioxidative protection, even though this was not captured in the *in vitro* antioxidant test. Moreover, as already mentioned, there are findings that suggest that excess of surfactant forms micelles in the aqueous phase which are able to encapsulate prooxidative species (McClements and Decker, 2000), therefore contributing to the antioxidant activity of the blank formulation. It should be emphasized that, in general, submicron entities possess enormous adsorbtion ability, offering additional pathway for removal of the free radicals (Bajić *et al*, 2017). Nevertheless, even though curcumin-loaded formulations provided higher number of both protected and repaired cells, *in vivo* study could be performed in order to detect some more pronounced beneficial effects of curcumin-loaded low-energy nanoemulsions and to capture the difference in the activity regarding curcumin's concentration.

4. Conclusion

In conclusion, the low-energy nanoemulsion formation via spontaneous emulsification was profoundly discussed in this work. It was demonstrated that, for the system consisting of Polysorbate 80 and soybean lecithin as surfactants, medium-chain triglycerides as the oil phase and ultra-pure water as the water phase, nanoemulsification process originates from a liquid crystalline state that arises at the border of organic and water phase, which eventually becomes dispersed into spherical nanodroplets. Morphology of inner phase was visualized through AFM.

Formulation with surfactant-to-oil ratio of 1 and 10% *w/w* of the oil was selected as the most suitable based on monitored physicochemical parameters. Upon the solubilization capacity for curcumin had been determined, three different concentration of curcumin were selected for further studies: 1, 2 and 3mg/mL. Both blank formulation and the curcumin-loaded ones exhibited small nanodroplets (110 – 135.5 nm) with uniform droplet size distribution after preparation. According to DSC analysis finding and microscopy, curcumin was completely solubilized in the formulations. Stability follow-up demonstrated promising results not only in terms of low-energy nanoemulsion formulations kinetic stability, but also in terms of chemical stability of encapsulated curcumin.

Safety profile screening through Comet assay suggested high biocompatibility of the blank and curcumin-loaded formulations. Preliminary biological activity evaluation of curcumin-loaded low-energy nanoemulsions pointed out their strong antioxidant potential, revealing both antigenotoxic properties - protective and reparative. This is very important if we have in mind that in the etiology of some specific skin-related disorders, such as photocarcinogenesis, the DNA mutations lie, which are caused by oxidative stress. Strong activity of curcumin involved in protection of cells against oxidative stress should be further exploited. In order to take the most of it, defying its underlined problematic properties, further experimental work should be devoted to collecting valuable information on performances of developed formulations in cell cultures, directing it to some more specific therapeutic implications, such as melanoma. Additionally, regarding potentials for dermal application of these formulations, *in vivo* dermatopharmakokinetinc profiling of curcumin from developed low-energy nanoemulsions should be assessed, as a relevant signal of curcumin's availability upon application. Also, more profound physicochemical evaluation, including drug-carrier interactions assessment, is to be

done.

5. *Conflict of interest*

The authors have no financial or non-financial interests that represent potential conflict of interests.

6. Acknowledgement

The authors are very grateful to the Ministry of Education, Science and Technological Development of the Republic of Serbia, for supporting this research within the framework of the project TR34031 – *Development of micro- and nanosystems as carriers for drugs with anti-inflammatory effect and methods for their characterization.* This work was also supported by the

bilateral project between the Republic of Serbia and the Federal Republic of Germany, named *Biosurfactants and biopolysaccharides/film-forming polymers as cosmetic raw materials and prospective pharmaceutical excipients: formulation of colloidal and film-forming delivery systems.* The authors are very grateful to the project OI 173034.

7. *References*

1. Aggarwal, B. B., Harikumar, K. B. (2009). Potential therapeutic effects of curcumin, the anti-inflammatory agent, against neurodegenerative, cardiovascular, pulmonary, metabolic, autoimmune and neoplastic diseases. *Int J Biochem Cell Biol, 41*(1), 40-59.

2. Anton, N. and Vandamme, T. F. (2009). Nano-emulsions and Micro-emulsions: Clarifications of the Critical Differences. *Pharm Res, 28*(5), 978–985.

3. Bajić, V., Spremo-Potparević, B., Živković, L., Čabarkapa, A., Kotur-Stevuljević, J., Isenović, E., Sredojević, D., Vukoje, I., Lazić, V., Ahrenkiel, S.P. Nedeljković, J. M. (2017). Surface-modified TiO2 nanoparticles with ascorbic acid: Antioxidant properties and efficiency against DNA damage in vitro. *Colloids Surf B Biointerfaces, 155*, 323-331.

4. Banerjee, S., Ji, C., Mayfield, J. E., Goel, A., Xiao, J., Dixon, J. E., Guo, X. (2018). Ancient drug curcumin impedes 26S proteasome activity by direct inhibition of dual-specificity tyrosine-regulated kinase 2. *PNAS*, 201806797

5. Banerjee, A., Kunwar, A., Mishra, B., Priyadarsini, K. I. (2008). Concentration dependent antioxidant/pro-oxidant activity of curcumin: Studies from AAPH induced hemolysis of RBCs. *Chem Biol Interact*, *174*(2), 134-139.

6. Benzie, I. F., Strain, J. J. (1999). Ferric reducing/antioxidant power assay: Direct measure of total antioxidant activity of biological fluids and modified version for simultaneous measurement of total antioxidant power and ascorbic acid concentration. *Methods Enzymol*. *299*, 15-27.

7. Blois, M. S. (1958). Antioxidant determinations by the use of a stable free radical. *Nature*, *181*(4617), 1199.

8. Buchanan, M., Egelhaaf, S. U., Cates, M. E. (2000). Dynamics of interface instabilities in nonionic lamellar phases. *Langmuir*, *16*(8), 3718-3726.

9. Chen, Y., Wu, Q., Zhang, Z., Yuan, L., Liu, X., Zhou, L. (2012). Preparation of

curcumin-loaded liposomes and evaluation of their skin permeation and pharmacodynamics. *Molecules*, *17*(5), 5972-5987.

10. Đekić, Lj. and Primorac, M. (2017). Microemulsion and Nanoemulsions as Carriers for Delivery of NSAIDs. In: *Microsized and Nanosized Carriers for Nonsteroidal Anti-Inflammatory Drugs - Formulation Challenges and Potential Benefit.* B. Čalija (ed.), 1st ed, Elsevier, Cambridge, MA, USA, pp. 69-94.
11. Fotticchia, T., Vecchione, R., Scognamiglio, P. L., Guarnieri, D., Calcagno, V., Di Natale, C., Attanasio, C., De Gregorio, M., Di Cicco, C., Quagliariello, V. Maurea, N., Barbieri, A., Arra, C., Raiola,L., Iaffaioli, R.V., Netti, A. P. (2017). Enhanced Drug Delivery into Cell Cytosol via Glycoprotein H-Derived Peptide Conjugated Nanoemulsions. *ACS Nano*, *11*(10), 9802-9813.
12. Ghanema, I. I. A., Sadek, K. M. (2012). Olive leaves extract restored the antioxidant perturbations in red blood cells hemolysate in streptozotocin induced diabetic rats. *International Journal of Biological, Biomolecular, Agricultural, Food and Biotechnological Engineering*, *6*(4), 124-130.
13. Gupta, S. C., Patchva, S., Aggarwal, B. B. (2013). Therapeutic roles of curcumin: lessons learned from clinical trials. *AAPS J*, *15*(1), 195-218.
14. Hatcher, H., Planalp, R., Cho, J., Torti, F. M., Torti, S. V. (2008). Curcumin: from ancient medicine to current clinical trials. *Cell Mol Life Sci*, *65*(11), 1631-1652.
15. Helgeson, M. E. (2016). Colloidal behavior of nanoemulsions: Interactions, structure, and rheology. *Cur Opin Colloid Interface Sci*, *25*, 39-50.

16. Isailović, T., Đorđević, S., Marković, B., Ranđelović, D., Cekić, N., Lukić, M., Pantelić, I., Daniels, R. and Savić, S. (2016). Biocompatible Nanoemulsions for Improved Aceclofenac Skin Delivery: Formulation Approach Using Combined Mixture-Process Experimental Design. *J Pharm Sci*, *105*(1), 306-323.

17. Isailović, T., Todosijević, M., Đorđević, S. and Savić, S (2017). Natural Surfactants-Based Micro/Nanoemulsion Systems for NSAIDs—Practical Formulation Approach, Physicochemical and Biopharmaceutical Characteristics/Performances. In: *Microsized and Nanosized Carriers for Nonsteroidal Anti-Inflammatory Drugs - Formulation Challenges and Potential Benefit.* B. Čalija (ed.), 1st edn, Elsevier, Cambridge, MA, USA, pp. 179-218.

18. Jacobs, C. and Müller, R.H. (2002). Production and characterization of a budesonide. *Pharm Res*, *19*(2), 189-194.

19. Jovanovic, S. V., Steenken, S., Boone, C. W., Simic, M. G. (1999). H-atom transfer is a preferred antioxidant mechanism of curcumin. *J Am Chem Soc*, *121*(41), 9677-9681.

20. Kablanov A. S. and Shchukin, E. D. (1992) Ostwald ripening theory: Applications to fluorocarbon emulsions. *Adv Colloid Interface Sci*, *38*, 69-97.

21. Kant, V., Gopal, A., Kumar, D., Pathak, N. N., Ram, M., Jangir, B. L., Tandan, S. K., Kumar, D. (2015). Curcumin-induced angiogenesis hastens wound healing in diabetic rats. *J Sur Res*, *193*(2), 978-988.

22. Kant, V., Gopal, A., Pathak, N. N., Kumar, P., Tandan, S. K., Kumar, D. (2014). Antioxidant and anti-inflammatory potential of curcumin accelerated the cutaneous wound healing in streptozotocin-induced diabetic rats. *Int Immunopharmacol*, *20*(2), 322-

330.

23. Klang, V. and Valenta, C. (2011). Lecithin-based nanoemulsions. *J Drug Deliv Sci Technol*, *21*(1), 55-76.

24. Komaiko, J. and McClements, D. J. (2014). Optimization of isothermal low-energy nanoemulsion formation: Hydrocarbon oil, non-ionic surfactant, and water systems. *J Colloid Interface Sci, 42*, 59-66.

25. Komaiko, J. S., and McClements, D. J. (2016). Formation of Food-Grade Nanoemulsions Using Low-Energy Preparation Methods: A Review of Available Methods. *Compr Rev Food Sci Food Saf*, *15*(2), 331-252.

26. Kumar, G., Mittal, S., Sak, K., Tuli, H. S. (2016). Molecular mechanisms underlying chemopreventive potential of curcumin: Current challenges and future perspectives. *Life Sci*, *148*, 313-328.

27. Li, J., Wang, X., Li, C., Fan, N., Wang, J., He, Z., Sun, J. (2017). Viewing molecular and interface interactions of curcumin amorphous solid dispersions for comprehending dissolution mechanisms. *Mol Pharm*, *14*(8), 2781-2792.

28. López-Montilla, J. C., Herrera-Morales, P. E., Pandey, S., Shah, D. O. (2002). Spontaneous emulsification: mechanisms, physicochemical aspects, modeling, and applications. *J Disper Sci Techno*l, *23*(1-3), 219-268.

29. McClements D. J. (2012). Nanoemulsions *versus* microemulsions: terminology, differences, and similarities. *Soft Matter, 8*(6), 1719-1729.

30. McClements, D. J., Decker, E. A. (2000). Lipid oxidation in oil- in- water emulsions: Impact of molecular environment on chemical reactions in heterogeneous food

systems. *JFS*, *65*(8), 1270-1282.

31. Mendonça, L. M., dos Santos, G. C., Antonucci, G. A., dos Santos, A. C., Bianchi, M. D. L. P., Antunes, L. M. G. (2009). Evaluation of the cytotoxicity and genotoxicity of curcumin in PC12 cells. *Mutat Res Genet Toxicol Environ Mutagen*, *675*(1), 29-34.

32. Mu, Q., Yu, J., McConnachie, L. A., Kraft, J. C., Gao, Y., Gulati, G. K., Ho, R. J. (2018). Translation of combination nanodrugs into nanomedicines: lessons learned and future outlook. *J Drug Target*, *26*(5-6), 435-447.

33. Müller, R. H., Harden, D., Keck, C. M. (2012). Development of industrially feasible concentrated 30% and 40% nanoemulsions for intravenous drug delivery. *Drug Dev Ind Pharm*, *38*(4), 420-430.

34. Neubert, R. H. (2011). Potentials of new nanocarriers for dermal and transdermal drug delivery. *Eur J Pharm Biopharm*. *77* (1), 1-2.

35. Pan, Y., Tikekar, R. V., Nitin, N. (2013). Effect of antioxidant properties of lecithin emulsifier on oxidative stability of encapsulated bioactive compounds. *Int J Pharm*, *450*(1-2), 129-137.

36. Pardeike, J. and Müller, R. H. (2010). Nanosuspensions: A promising formulation for the new phospholipase A2 inhibitor PX-18. *Int J Pharm, 391*(1-2), 322-329.

37. Quian, C. and McClements, D. J. (2011). Formation of nanoemulsions stabilized by model food-grade emulsifiers using high-pressure homogenization: Factors affecting particle size. *Food Hydrocoll, 25*(5), 1000-1008.

38. Saberi, A. H., Fang, Y., McClements, D. J. (2013). Fabrication of vitamin E-enriched nanoemulsions: factors affecting particle size using spontaneous emulsification. *J*

Colloid Interface Sci, *391*, 95-102.

39. Santana, R. C., Fasolin, L.H. and De Cunha, R. L. (2012). Effects of a cosurfactant on the shear-dependent structures of systems composed of biocompatible ingredients. *Colloids Surf A Physicochem Eng Asp*, *398*, 54-63.

40. Sebastià, N., Soriano, J. M., Barquinero, J. F., Villaescusa, J. I., Almonacid, M., Cervera, J., Such, E., Silla M. A., Montoro, A. (2012). In vitro cytogenetic and genotoxic effects of curcumin on human peripheral blood lymphocytes. *Food Chem Toxicol*, *50*(9), 3229-3233.

41. Seca, A. M., Pinto, D. C. (2018). Plant Secondary Metabolites as Anticancer Agents: Successes in Clinical Trials and Therapeutic Application. *Int J Mol Sci, 19*(1), 263.

42. Shah, V. P., Yacobi, A., Rădulescu, F. Ş., Miron, D. S., Lane, M. E. (2015). A science based approach to topical drug classification system (TCS). *Int J Pharm*, *491*(1-2), 21-25.

43. Sharma, R. A., Gescher, A. J. and Steward, W. P. (2005). Curcumin: The story so far. *Eur J Cancer*, *41*(13), 1955–1968.

44. Singh, Y., Meher, J. G., Raval, K., Khan, F. A., Chaurasia, M., Jain, N. K., Chourasia, M. K. (2017). Nanoemulsion: Concepts, development and applications in drug delivery. *J Control Release, 252*, 28-49.

45. Sreekanth, V., Bajaj, A. (2013). Number of free hydroxyl groups on bile acid phospholipids determines the fluidity and hydration of model membranes. *J Phys Chem* B, *117*(40), 12135-12144.

46. Tadros, T., Izquierdo, P., Esquena, J. and Solans C. (2004). Formation and stability of

nano-emulsions. *Adv Colloid Interface Sci, 108 –109*, 303–318.

47. Taylor, P. (1998) Ostwald ripening in emulsions. *Adv Colloid Interface Sci, 75*, 107-163.

48. Thangapazham, R. L., Sharma, A., Maheshwari, R. K. (2006). Multiple molecular targets in cancer chemoprevention by curcumin. *AAPS J, 8*(3), E443.

49. Todosijević, M. N., Cekić, N. D., Savić, M. M., Gašperlin, M., Ranđelović, D. V., Savić, S. D. (2014). Sucrose ester-based biocompatible microemulsions as vehicles for aceclofenac as a model drug: formulation approach using D-optimal mixture design. *Colloid Polym Sci, 292*(12), 3061-3076.

50. Uson, N., Garcia, M. J., Solans, C. (2004). Formation of water-in-oil (W/O) nano-emulsions in a water/mixed non-ionic surfactant/oil systems prepared by a low-energy emulsification method. *Colloids Surf A Physicochem Eng Asp, 250*(1-3), 415-421.

51. Valko, M., Rhodes, C., Moncol, J., Izakovic, M. M., Mazur, M. (2006). Free radicals, metals and antioxidants in oxidative stress-induced cancer. *Chem-Biol Interact, 160*(1), 1-40.

52. Vecchione, R., Quagliariello, V., Calabria, D., Calcagno, V., De Luca, E., Iaffaioli, R. V., Netti, P. A. (2016). Curcumin bioavailability from oil in water nano-emulsions: In vitro and in vivo study on the dimensional, compositional and interactional dependence. *Journal Control release, 233*, 88-100.

53. Villegas, I., Sánchez- Fidalgo, S., Alarcón de la Lastra, C. (2008). New mechanisms and therapeutic potential of curcumin for colorectal cancer. *Mol Nutr Food Res, 52*(9), 1040-1061.

54. Wang, Y. J., Pan, M. H., Cheng, A. L., Lin, L. I., Ho, Y. S., Hsieh, C. Y., Lin, J. K. (1997). Stability of curcumin in buffer solutions and characterization of its degradation products. *J Pharm Biomed Anal*, *15*(12), 1867-1876.

55. Wooster, T. J., Golding, M. and Sanguansri, P. (2008) Impact of Oil Type on Nanoemulsion Formation and Ostwald Ripening Stability. *Langumin*, *24*(22), 12758-12765.

56. Wright, T. I., Spencer, J. M., Flowers, F. P. (2006). Chemoprevention of nonmelanoma skin cancer. *J Am Acad Dermatol*, *54*(6), 933-946.

57. Yallapu, M. M, Jaggi, M., Chauhan, S. C. (2012). Curcumin nanoformulations: a future nanomedicine for cancer. *Drug Discov Today*, *17* (1-2), 71-80.

58. Yallapu, M. M., Bhusetty Nagesh, P. K., Jaggi, M. and Chauhan, S. C. (2015). Therapeutic Applications of Curcumin Nanoformulations. *AAPS J*, *17*(6), 1341-1355.

59. Zugic, A., Jeremic, I., Isakovic, A., Arsic, I., Savic, S., Tadic, V. (2016). Evaluation of Anticancer and Antioxidant Activity of a Commercially Available CO2 Supercritical Extract of Old Man's Beard (Usnea barbata). *PloS one*, *11*(1), 1-13.

60. Žukovec Topalović, D., Živković, L., Čabarkapa, A., Djelić, N., Bajić, V., Dekanski, D., Spremo-Potparević, B. (2015). Dry olive leaf extract counteracts L-thyroxine-induced genotoxicity in human peripheral blood leukocytes in vitro. *Oxid Med Cell Longev, 2015,* 1-8.

Figure 1. Formulations with different SOR values: Formulations with SORs from 0.75 to 4 represent low-energy nanoemulsions with 10 % *w/w* of the oil phase, and the last one is a microemulsion obtained for the highest SOR ratio

Figure 2. a) Anisotropic structures formed at the contact surface of oil, water and surfactants; b) AFM images of oil-water-surfactant contact – 2D image (left) and 3D image – topography (right)

Figure 3. a) Electrical conductivity for the SOR 1 mixture with different water content; b) Rheological behavior of the samples with SOR 1, with 60, 70 and 80 % w/w of water

Figure 4. a) DSC thermograms in cooling mode for SOR 1 mixture with different water ratios; b) thermograms of the F1 and curcumin-loaded formulations, c) thermogram of ultra-purified water – heating mode

Figure 5. AFM images of the F1 formulation: 2D image (left) and 3D image (right)

Figure 6. Curcumin-loaded formulations: a) stable formulations, without precipitation; b) formulations that exhibited precipitation (left: 4mg/mL of curcumin; right: 5 mg/mL of curcumin

Figure 7. *In vitro* release results for curcumin from selected formulations

Figure 8. Chemical stability of curcumin in the formulations during 3 months

Figure 9. a) DPPH absorbance decay with increase in the antioxidant concentration; b) Free radical scavenging activity in the function of antioxidant concentration (DPPH assay); c) FRAP assay results; $^{*}p<0.05$, compared with tocopherol

Figure 10. a) Genotoxicity evaluation of developed formulations: $^{*}p<0.05$ versus H_2O_2, $^{\#}p<0.05$ versus F1; b) Protective antigenotoxic potential of developed formulations: $^{*}p<0.05$ versus H_2O_2; c) Reparative antigenotoxic potential of developed formulations: $^{*}p<0.05$ versus H_2O_2

Table 1. Summarized properties of selected low-energy nanoemulsions

SOR	Oil content (% w/w)	Z-ave (nm)	PDI	pH
0.75	10	140.0±4.2	0.191±0.11	4.35±0.01
1	10	107.43±1.47	0.165±0.018	4.78±0.05
1.5	10	100.6±2.74	0.250±0.15	5.3±0.1
2	10	92.21±3.29	0.310±0.005	6.81±0.1
4	10	52.83±4.74	0.392±0.11	7.1±0.1

1085 Table 2. Qualitative and quantitative composition of the F1 and corresponding curcumin-loaded formulations

Formulation	**Composition (% *w/w*)**				
	MCT	**P80**	**Le**	**CU**	**W**
F1	10	9	1	/	80
F1_CU_1	10	9	1	0.1	79.9
F1_CU_2	10	9	1	0.2	79.8
F1_CU_3	10	9	1	0.3	79.7

Table 3. Comparative physicochemical properties of the blank and curcumin-loaded formulation

	Size (nm)	PDI	ZP (mV)	pH	EC (µS/cm)	Viscosity
F1	110.43±1.47	0.165±0.018	-30.33±1.81	4.78±0.05	116.9±0.9	3.13±0.07
F1_CU_1	121.4±2.4$^{*\#}$	0.176±0.016	-25.2±1.5*	5.6±0.1*	93.1±0.02*	3.19±0.04*
F1_CU_2	129.3±0.9$^{*\#}$	0.172±0.01	-22.1±1.1*	5.7±0.1*	93.2±0.5*	2.92±0.03*
F1_CU_3	135.5±2.3$^{*\#}$	0.187±0.012	-21.9±1.3*	5.7±0.05*	94.43±2.31*	2.97±0.03*

$^{*}p<0.05$, compared with the F1; $^{\#}p<0.05$, compared with other curcumin-loaded formulations

Table 4. Monitored physicochemical parameters after 3-months storage period

	Size (nm)	**PDI**	**ZP (mV)**	**pH**	**EC (µS/cm)**
F1	111.3±1.73	0.156±0.019	-25.7±1.1	4.73±0.1	97.1±5.1*
F_CU_1	126±1.5	0.158±0.006	-26.9±0.8	5.65±0.01	95.87±0.02
F_CU_2	131.2±1.6	0.165±0.013	-21.3±1.2	5.75±0.05	93.2±0.5
F_CU_3	146.8±0.8	0.175±0.015	-22.7±1.5	5.73±0.05	95.1±0.9

*$p<0.05$, compared with the same sample freshly prepared

1100

Figure 1

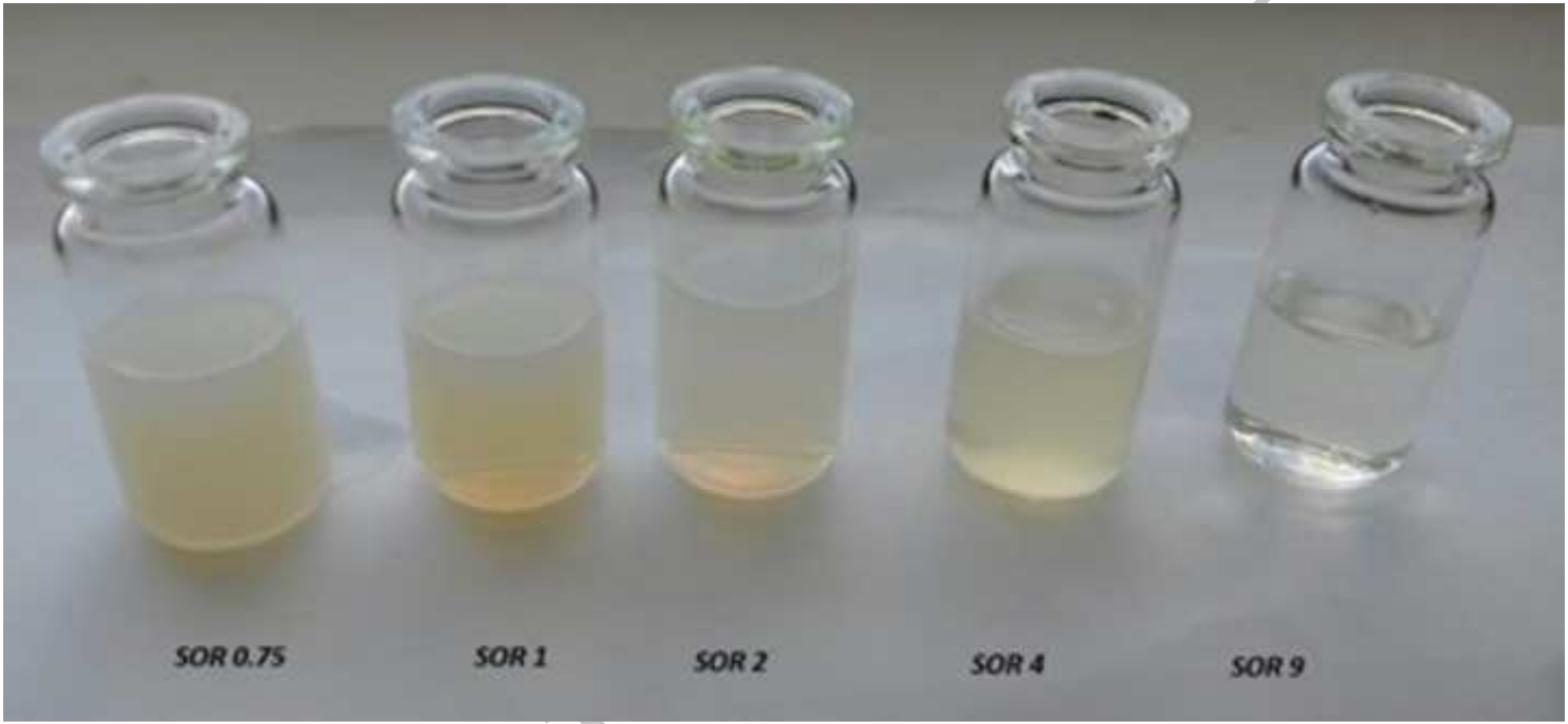

Figure 2

a)

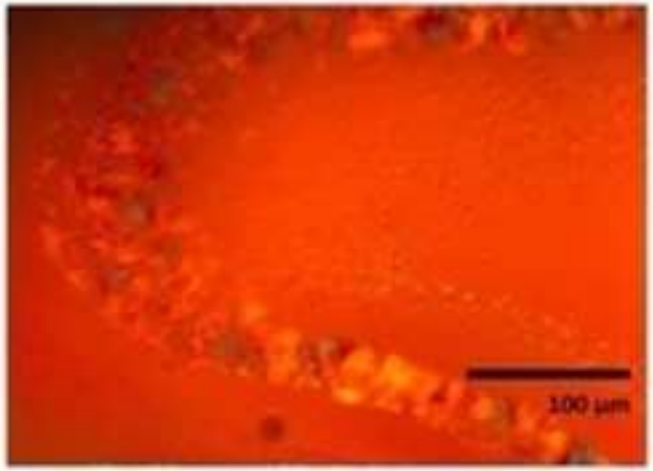

b)

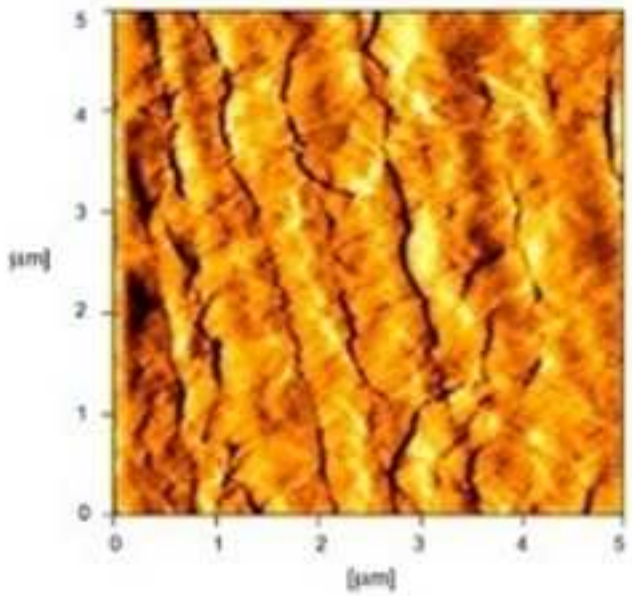

Figure 3

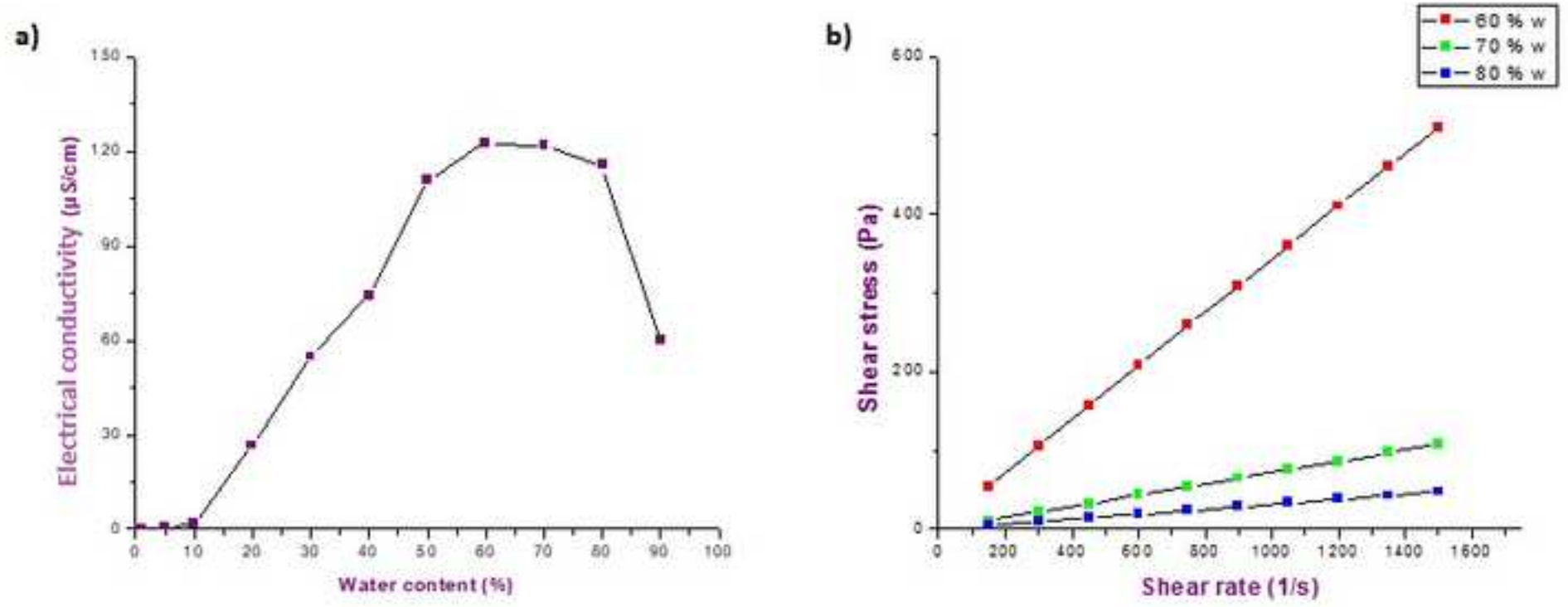

Figure 4

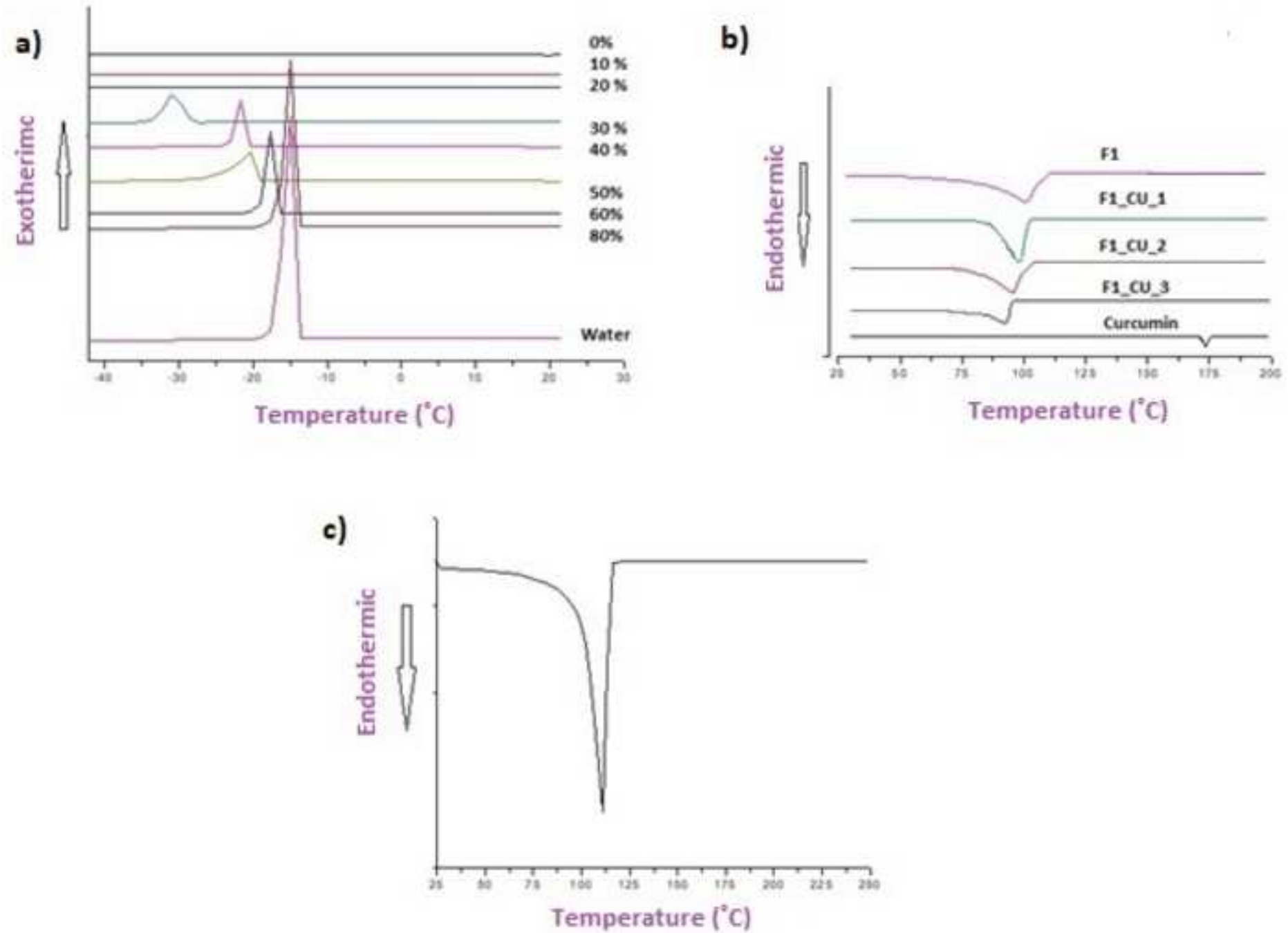

Figure 5

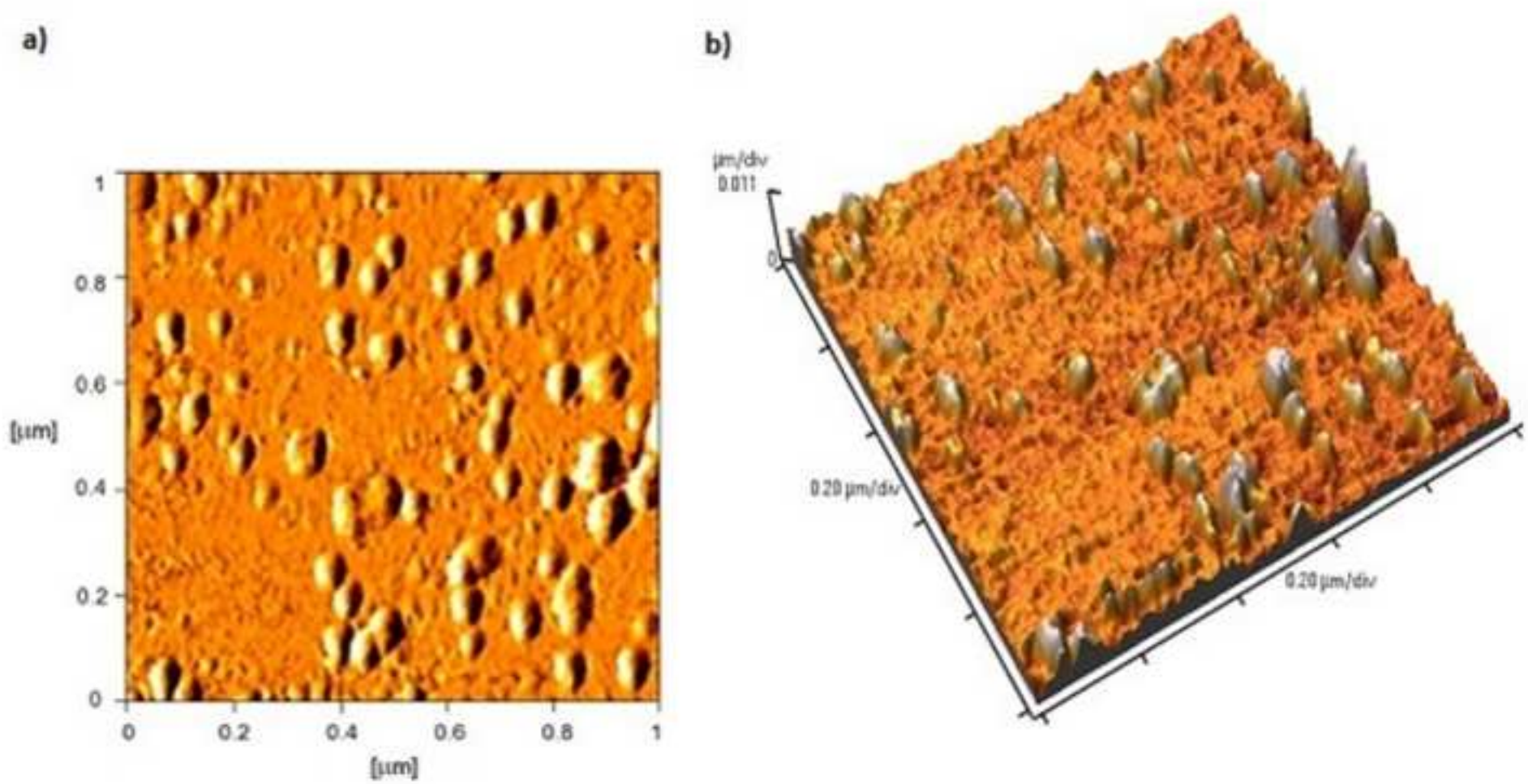

Figure 6

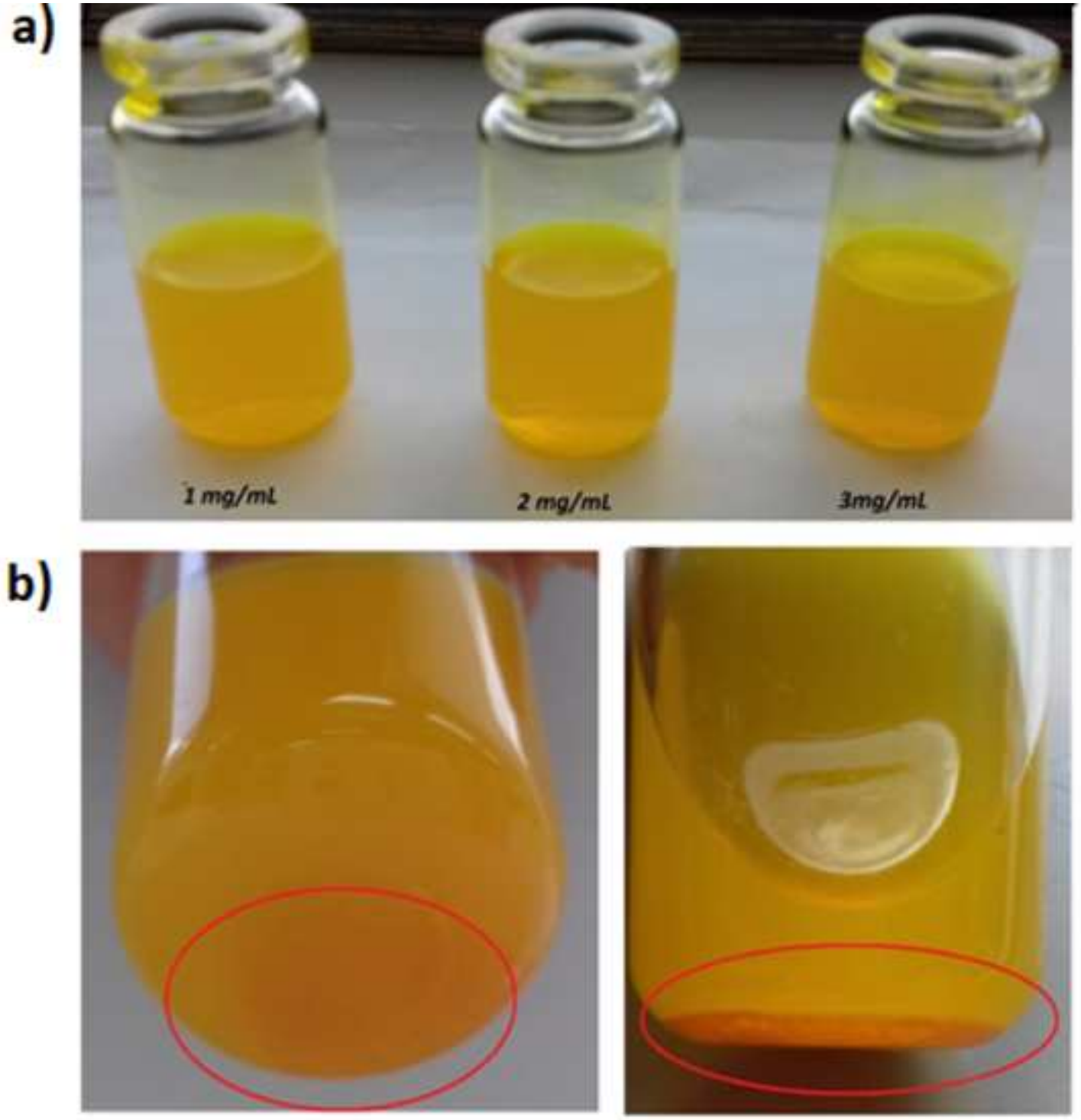

Figure 7

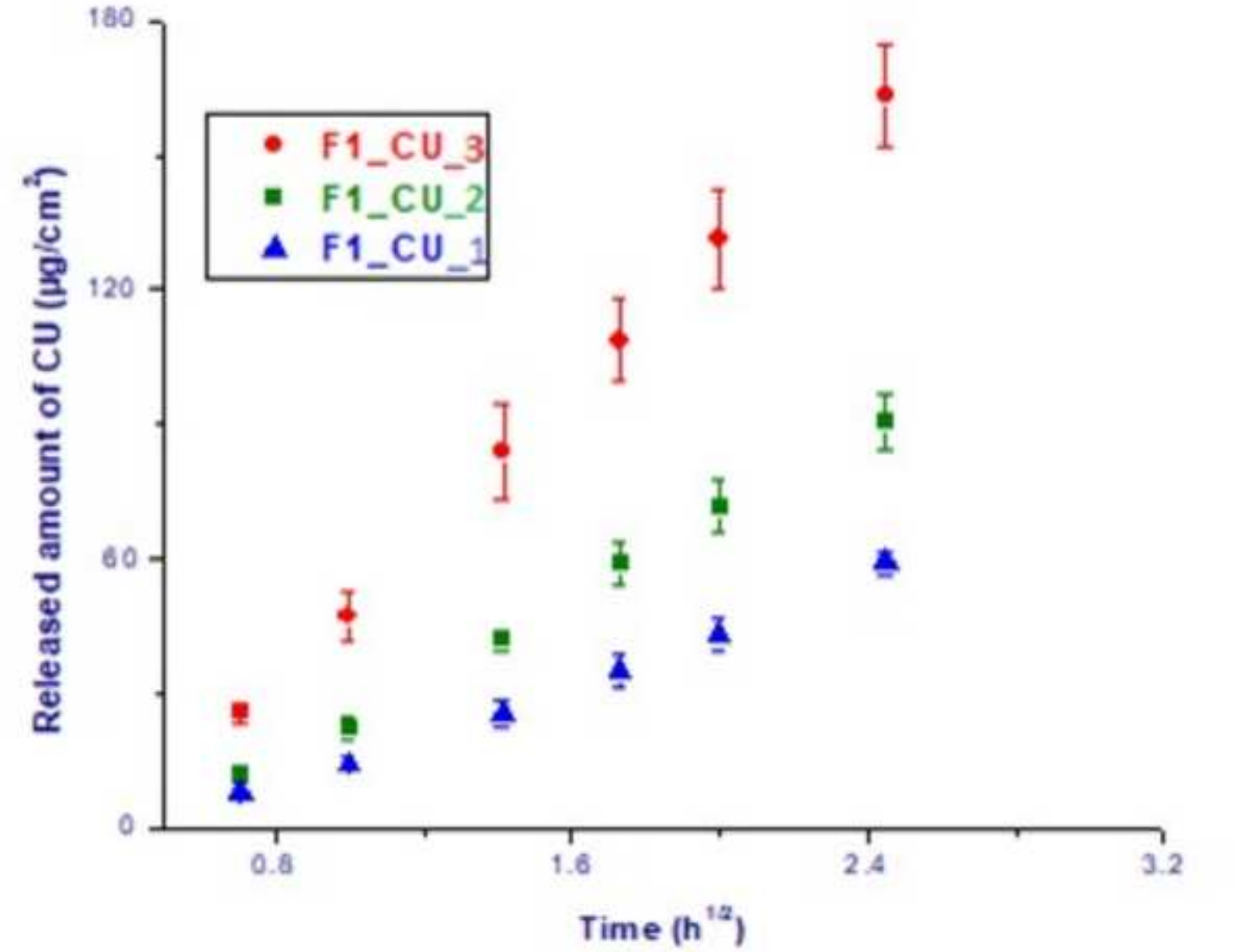

Figure 8

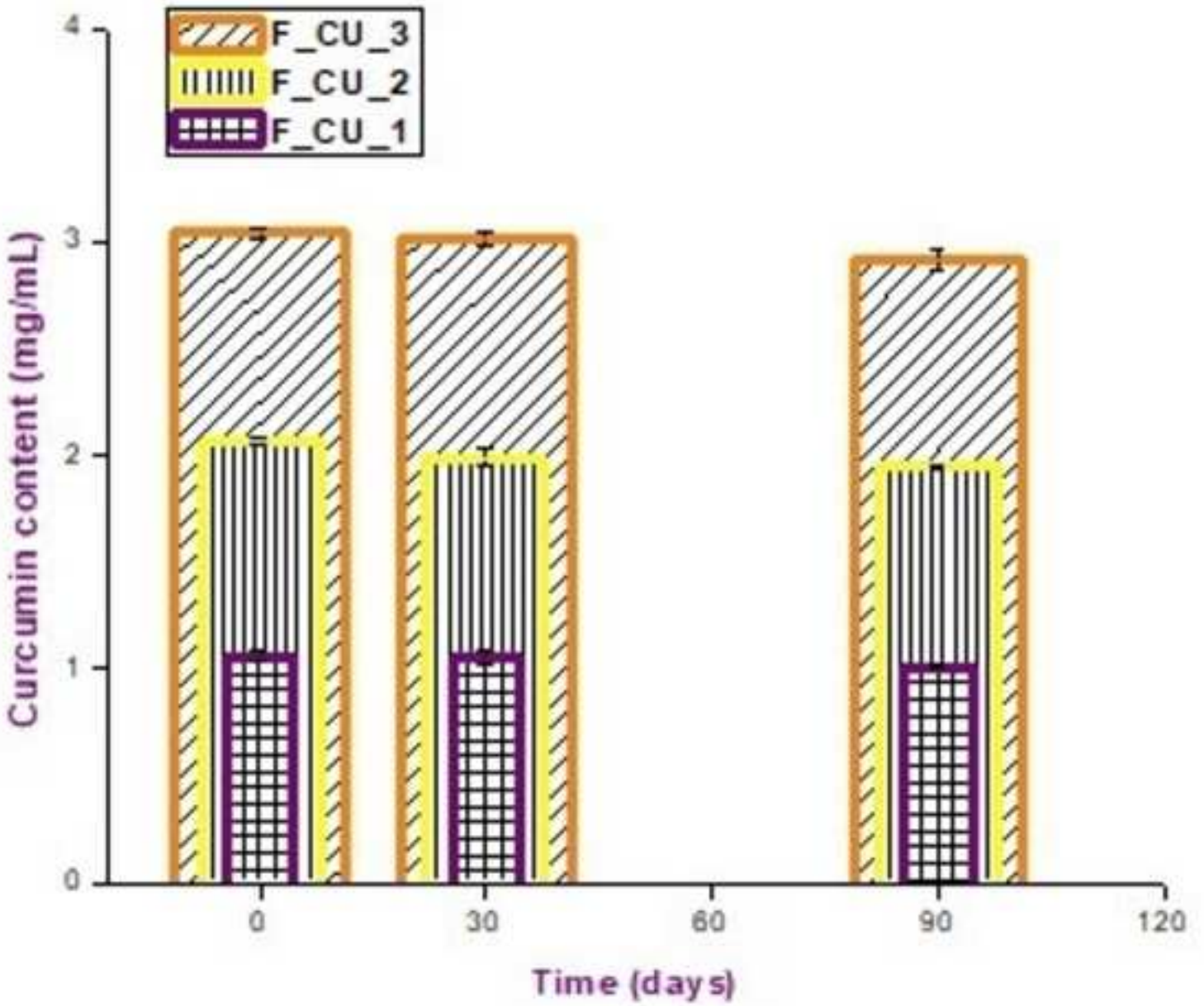

Figure 9

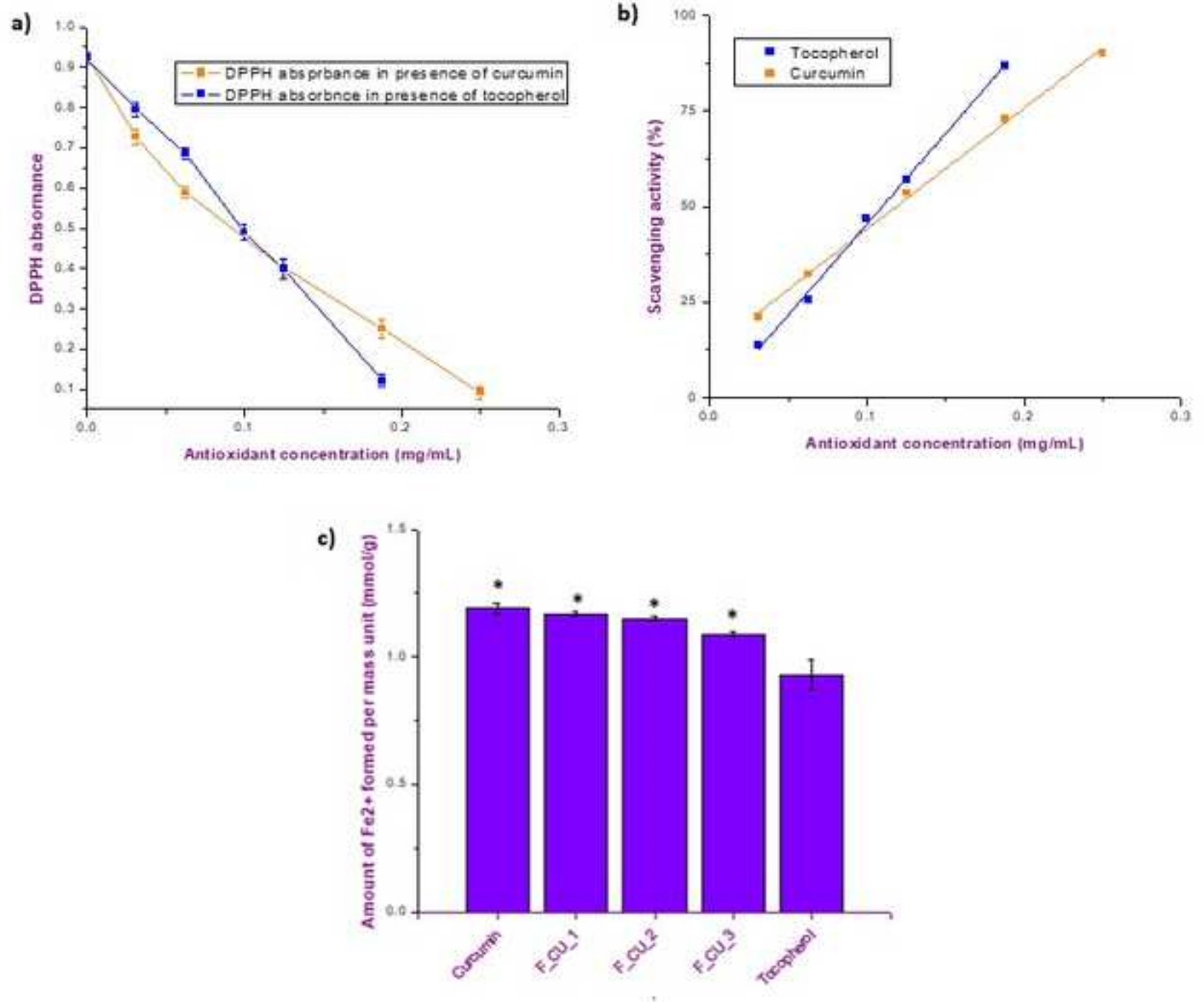

Figure 10